CAHIER SCIENTIFIQUE
REVUE TECHNIQUE LUXEMBOURGEOISE

CAHIER SCIENTIFIQUE BIANNUEL DE LA REVUE TECHNIQUE LUXEMBOURGEOISE 2 | 2014

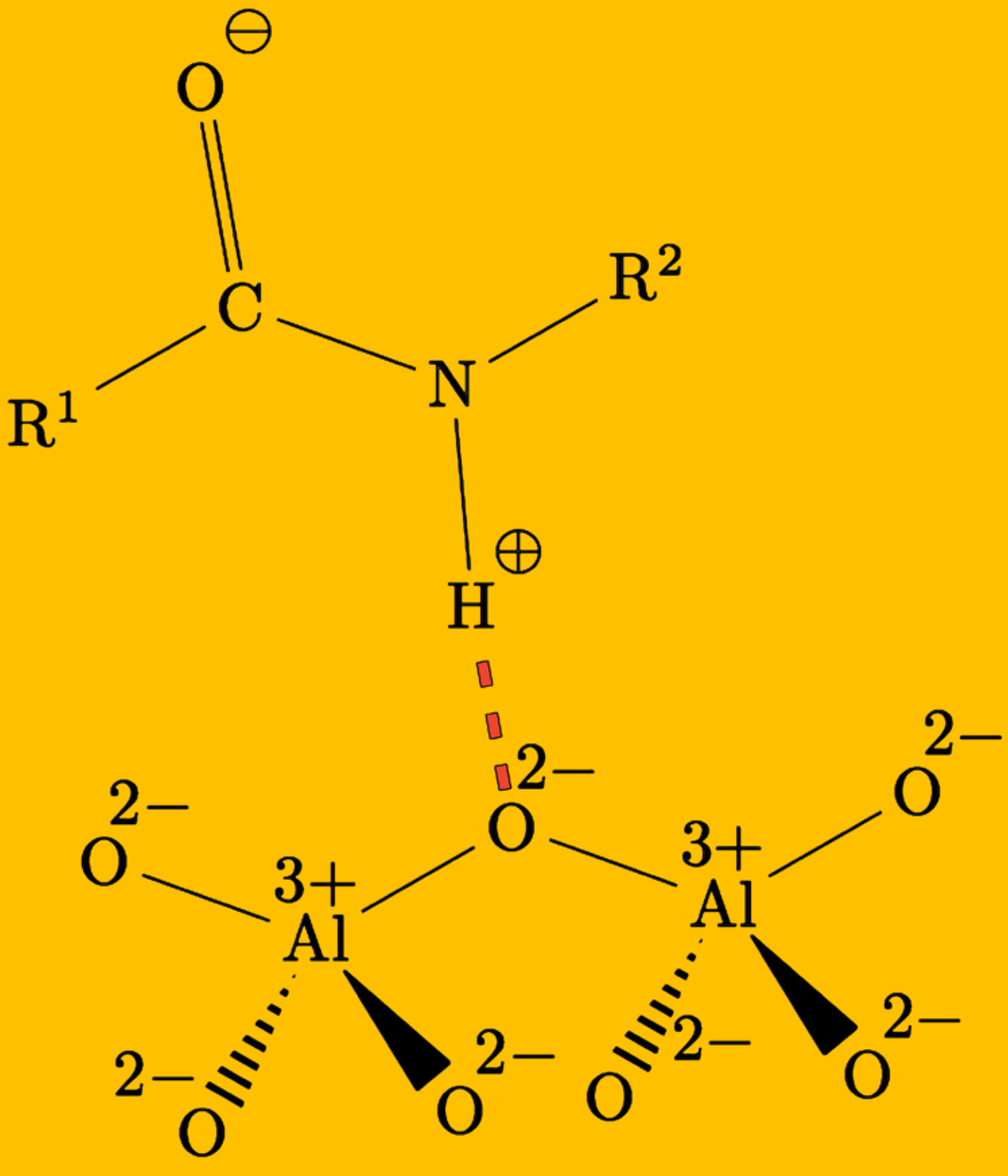

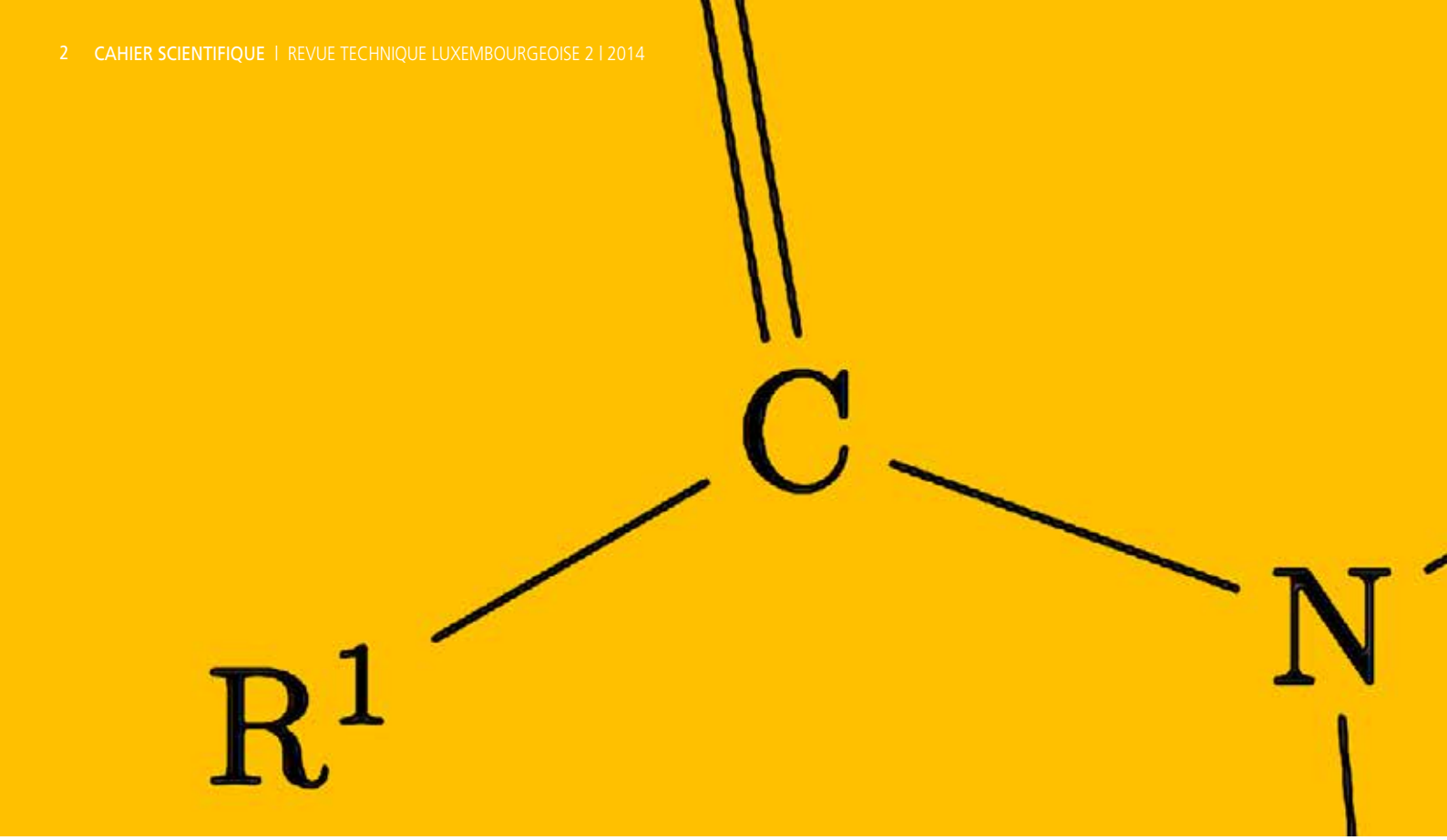

REVUE TECHNIQUE LUXEMBOURGEOISE

www.revue-technique.lu

pour

L'Association Luxembourgeoise des Ingénieurs, Architectes et Industriels

éditée par

Responsable Revue Technique Sonja Reichert
Graphisme Jan Heinze
t 45 13 54 23 s.reichert@revue-technique.lu
6, bv. G. D. Charlotte L-1330 Luxembourg

Impression 3.500 exemplaires
imprimerie HENGEN
14, rue Robert Stumper L-1018 Luxembourg

EDITO_

En tant qu'ancienne importante nation industrielle, le Luxembourg a aujourd'hui besoin de promouvoir la formation de l'ingénieur. En effet, la désindustrialision de ces dernières décennies a rendu l'ingénieur moins visible dans notre société.
De nos jours, on constate que cette désindustrialisation a rendu le marché du travail de notre pays plus vulnérable. L'industrie, créatrice de nombreux et de divers genres d'emplois a besoin d'ingénieurs pour encadrer et assurer la production ainsi que la gestion de l'entreprise.
Les jeunes faisant le choix de leurs études connaissent peu les possibilités que le métier de l'ingénieur offre et ne prennent souvent pas en compte cette formation. Le «Prix de la Revue Technique Luxembourgeoise» ainsi que le «Prix d'excellence», qui ont pour but de valoriser les études et carrières professionnelles de l'ingénieur, donnent la possibilité de présenter les aspects très variés des études et des tâches de l'ingénieur. Les publications de ces prix peuvent aider et guider les futurs étudiants dans l'orientation de leurs choix.

Le «Prix de la Revue Technique Luxembourgeoise 2014» émis par la Revue Technique luxembourgeoise, article du lauréat repris dans ce Cahier scientifique 02/2014 et le «Prix d'excellence 2013» émis par la Fondation Enovos, les travaux des participants publiés dans la Hors-série 010, ces prix sont une des raisons principales de mettre en évidence le «métier d'ingénieur» au début du 21ème siècle.

Michel Pundel
Président du jury du Prix d'Excellence

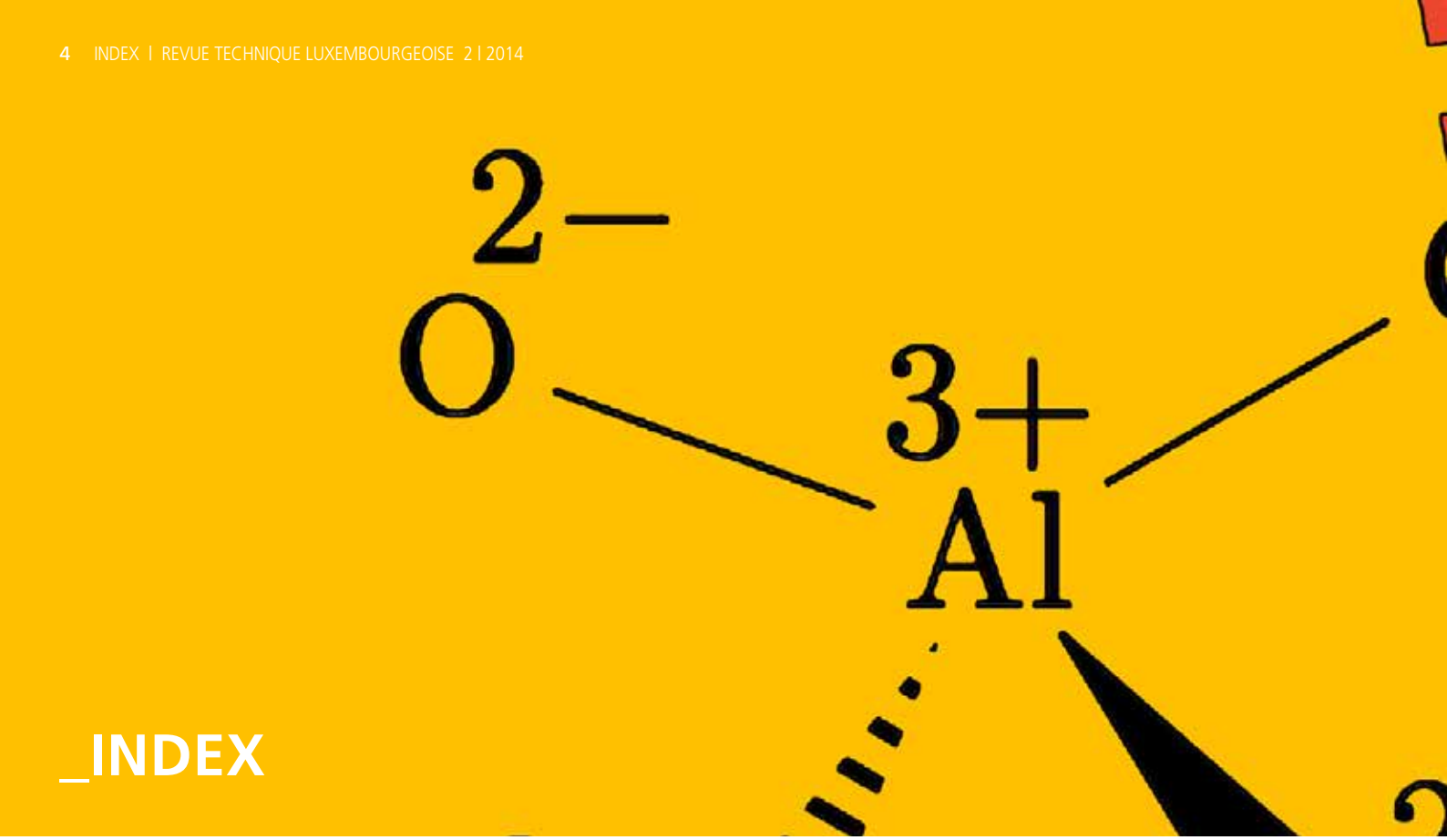

_INDEX

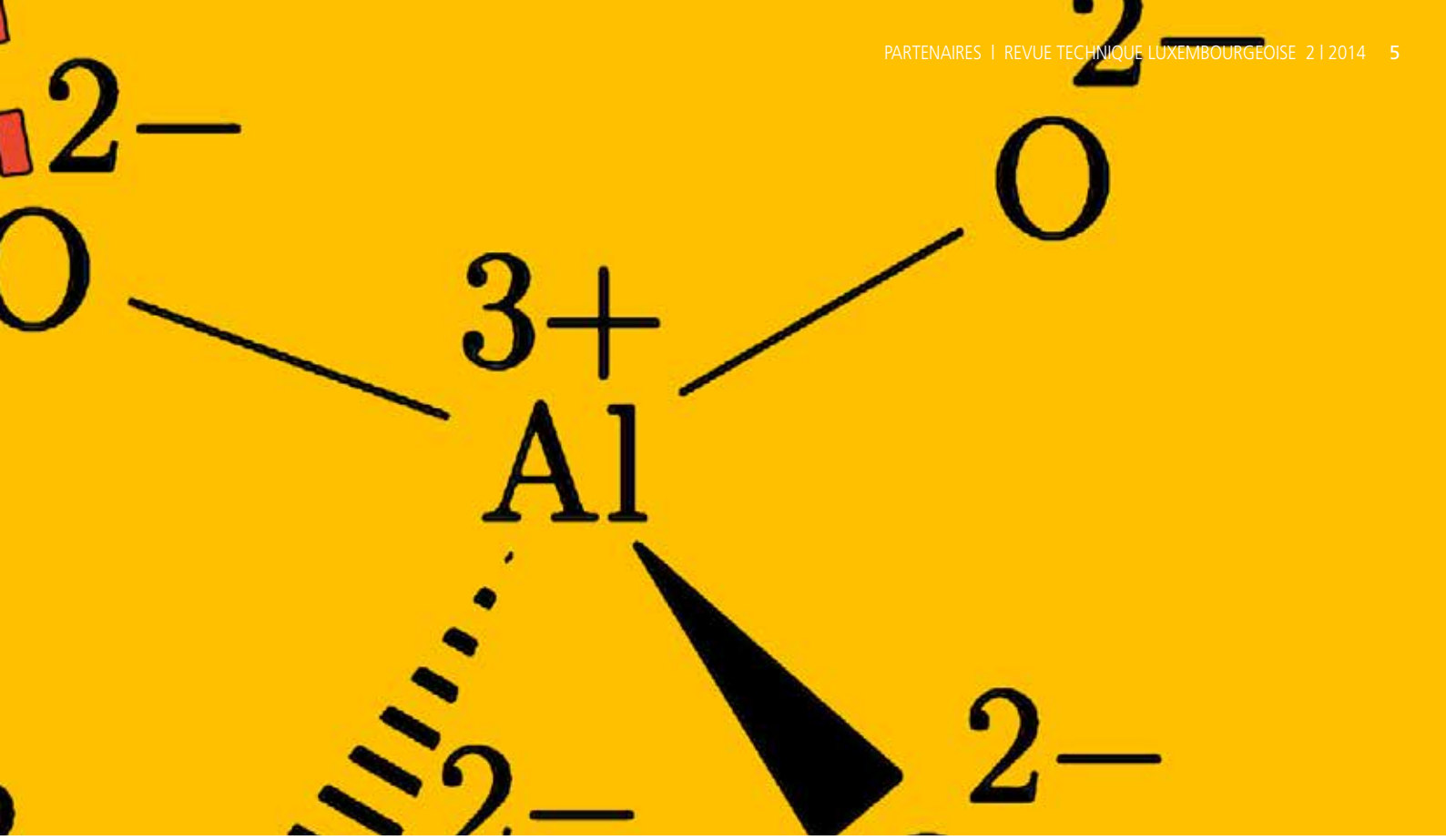

revue publiée pour_

www.ali.lu www.oai.lu www.tema.lu

ALIAI
ASSOCIATION LUXEMBOURGEOISE DES INGÉNIEURS - ARCHITECTES - INDUSTRIELS
www.aliai.lu

partenaires de la revue_

Fonds National de la Recherche Luxembourg
Luxembourg Institute of Science and Technology LIST
Chaux de Contern Groupe Eurobéton
CBL
GEBERIT
CDCL
Post Luxembourg
Prefalux
National Agency for Innovation and Research LUXINNOVATION
SOLUDEC
HENGEN Print & More
BAATZ Genie Civil Constructions
ANNEN
KELLER Wintergardens & Windows
PAUL WURTH SMS group
ArcelorMittal
OST manufaktur
steffen holzbau s.a.
KUHN Construction
uni.lu Université du Luxembourg
SECOLUX
GOODYEAR
Cimalux Ciments & Matériaux
BUROtrend Mobilier et installations de bureaux
MERSCH SCHMITZ

revue imprimée sur du papier_

HE PRINTED IN LUXEMBOURG
FSC MIXTE Papier issu de sources responsables FSC® C023609

Derzeitige energie- und klimapolitische Ziele der EU, definiert in der Strategie „Europa 2020", haben als höchste Priorität, intelligentes, nachhaltiges und integratives Wachstum Europas zu fördern. Die Stärkung der Nutzung von erneuerbaren Energien, einschließlich der Biomasse, ist heutzutage in allen Europäischen Ländern ein wichtiger Bestandteil der nationalen Strategien. Eine wichtige Technologie zur Energiegewinnung aus Biomasse ist die Biogserzeugung. In bestimmten Fällen kann diese „grüne" Energieproduktion allerdings auch Probleme verursachen, wie z.B. die Aufkonzentrierung von Gärresten und damit Nähstoffen, auf Ackerflächen in Gebieten die an Nährstoffüberschüssen leiden. In diesem Kontext soll das ARBOR Projekt dazu beitragen, regionale Pilotprojekte zu entwickeln, sowie eine überregionale Umsetzungsstrategie für eine nachhaltige Biomassenutzung zu etablieren. Dieser Artikel stellt Ergebnisse einer ökonomischen und ökologischen Bewertung verschiedener Gärrestbehandlungsanlagen in Flandern (Belgien) vor, die Wissenschaftler des Luxembourg Institute of Science and Technology (LIST) im Rahmen des Interreg IVB Projektes ARBOR durchgeführt haben.

Ökonomische und ökologische Auswertung

BEHANDLUNG VON GÄRRESTEN IN FLANDERN_

Dr.-Ing. Katarzyna Golkowska, Dipl.-Ing. (FH) Daniel Koster

Regionale Nährstoffüberschüsse erfordern neue Ansätze im Umgang mit Gärresten

Die Biogasanlagendichte in Europa ist über die letzten Jahre stark gestiegen. Die Biogasanalgen in manchen Europäischen Ländern, wie Deutschland, Italien oder Belgien sind zum festen Bestandteil der Agrarlandschaft geworden (BMU, 2009; Fabbri et al., 2010). In den Jahren 2006-2009 hat sich die jährliche Biogasproduktion in der EU insgesamt von 4899 auf 8346 kTÖE verdoppelt (EUROBSERV'ER, 2008; 2010). Die Biogasanlagen produzieren neben dem Biogas auch einen Gärrest - ein Rückstand der die Anlagen verlässt und meist als landwirtschaftlicher Dünger auf den Feldern verteilt wird da er einen hohen Anteil an Nährstoffen (u.a. Stickstoff- und Phosphorverbindungen) enthält. Die Konzentrierung von Biogasanlagen, die Energiepflanzen und organische Abfälle verarbeiten, in den Regionen, in denen intensive Landwirtschaft betrieben wird, kann zu lokalen Problemen mit überschüssigen Gärrestmengen führen. In solchen Regionen entstehen oft neue Gefährdungen für die Umwelt, die durch Nährstoffüberschüsse in landwirtschaftlichen Böden verursacht werden (Prapaspongsa et al. 2010; Rehl and Müller, 2011). Ein solches Szenario realisiert sich gerade in manchen landwirtschaftlichen Regionen Europas, wie z.B. in Flandern (Belgien), den Niederlanden, bzw. manchen Teilen Italiens und Deutschlands (Brouwer et al., 1999). Demzufolge wird die Gärrestbehandlung immer öfters angewendet, um die Umwelteinflüsse durch Nährstoffüberschuss auf den Feldern zu reduzieren (Lebuf et al., 2012).

Gärrestbehandlung – was spricht dafür?

Die Gärrestbehandlung in den Regionen mit einem Nährstoffüberschuss in den Böden ermöglicht die Reduzierung des Wassergehalts mancher Produkte, wodurch sie einfacher transportierbar werden. Außerdem können durch eine weitere Behandlung die NPK Flüsse (Nähstoffflüsse an Stickstoff, Phosphor und Kalium) getrennt und dadurch in einem begrenzten Ausmaß durch selektive Nutzung der Behandlungsprodukte steuerbar werden. Ein weiterer Vorteil ist die Möglichkeit starker Reduzierung der Direktemissionen, die mit der Ausbringen von Rohgärresten verbunden sind (Holm-Nielsen et al., 2009; Golkowska et al., 2012; Vázquez-Rowe et al. 2013). Auch das Nährstoffrecycling von Gärresten wird immer wichtiger für die Düngemittelindustrie - eine sehr energieintensive Branche, die stark unter unstabilen Preisen fossiler Brennstoffe leidet und zusätzlich künftig durch die Ausschöpfung von natürlichen Phosphorvorkommen betroffen sein wird (Fixen und Johnston, 2012). Diese Studie, erstellt im Rahmen des ARBOR-Projektes (INTERRREG IVB NWE), soll in diesem Zusammenhang bei der Suche nach nachhaltigen Konzepten für die Gärrestbehandlung helfen.

Vier alternative Behandlungssysteme im Überblick

Die durchgeführte ökologische und ökonomische Bewertung basiert auf Daten von drei existierenden Flämischen Gärrestbehandlungsanlagen, die vom Flämischen Koordinationszentrum für Mistverarbeitung (VCM) bereitgestellt wurden. Diese Analysen wurden durch eine ganze Reihe von Annahmen (z.B. für Gärrestcharakteristik, Energieversorgung, Transport, Ausbringung), sowie durch ein zusätzliches theoretisches Behandlungsszenario (betrachtet als künftige Alternative und nicht berücksichtigt in der ökonomischen Auswertung) ergänzt, um eine bessere Transparenz und Übertragbarkeit auf andere Regionen Europas zu gewährleisten. Insgesamt wurden vier verschiedene Technologien bewertet:

(A) Kompostierung der Gärreste
(B) Trocknen und anschließendes Pelletieren der Gärreste
(C) Ammoniak-Strippen und Trocknen
(D) Biologischer Stickstoffabbau, Umkehrosmose und Trocknen

Die ökobilanzielle Betrachtung umfasste jeweils die Behandlung des Eingangsgärrests in der Anlage aber auch Transport und Ausbringung des behandelten Gärrests auf die Felder. Als Basisvergleichsszenario wurde das direkte Ausbringen von unbehandelten Gärresten auf die landwirtschaftlichen Flächen analysiert. Da sich die Eigenschaften der Eingangsgärreste für die verschiedenen Anlagen stark voneinander unterscheiden, wurden die Analysen in 3 Gruppen aufgeteilt (s. Abbildung 1).

Ergebnisse der Ökobilanzierung

Die Ökobilanzierung soll eine Antwort liefern, ob unter gegebenen Bedingungen, die Behandlung von Gärresten und anschließendes Ausbringen auf die Felder, Vorteile gegenüber dem direkten Ausbringen auf die Felder bringt. Es handelt sich dabei um einen Vergleich zwischen verschiedenen Technologien. Die Behandlungsprodukte werden zwar innerhalb der Szenarien auf die Felder ausgebracht, allerdings wurde in der Analyse der Ersatz anderer Produkte nicht miteingerechnet, falls man mit den Gärrestbehandlungsprodukten die klassischen Düngemittel ersetzen würde. Auch die zu erwartenden Markteffekte die aus solchem Ersatz im großen Maßstab resultieren würden, wurden nicht berücksichtigt. Mehr Details über

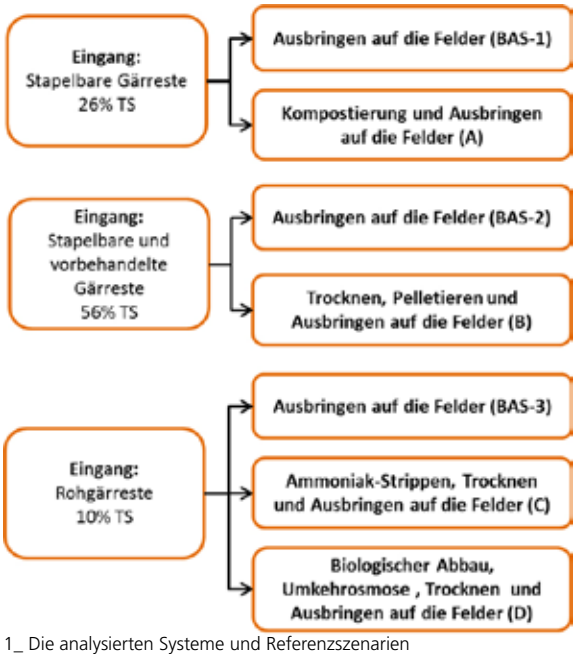

1_ Die analysierten Systeme und Referenzszenarien

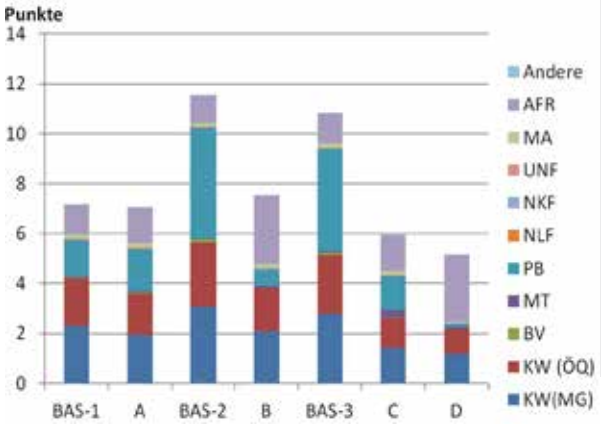

2_ Ergebnisse der Ökobilanzierung für die analysierten Systeme und Vergleichsszenarien; AFR – Abbau fossiler Ressourcen, MA – Metallabbau, UNF – Umwandlung von natürlichen Flächen, NKF – Nutzung von Siedlungsflächen, NLF – Nutzung von landwirtschaftlichen Flächen, PB – Partikelbildung, MT – menschliche Toxizität, BV – Bodenversauerung, KW(ÖQ) – Klimawandel Ökosystemqualität, KW(MG) – Klimawandel menschliche Gesundheit (Vázquez-Rowe et al., 2015)

Übersicht der Szenarien:

(BAS-1) Ausbringung der Gärreste (26 % TS)

(A) Kompostierung

(BAS-2) Ausbringung der Gärreste (56 % TS)

(B) Trocknen und Pelletieren

(BAS-3) Ausbringung der Gärreste (10 % TS)

(C) Ammoniak-Strippen und Trocknen

(D) Biologischer Stickstoffabbau, Umkehrosmose und Trocknen

die Untersuchungsmethodologie, sowie die Inputdaten und Annahmen sind in den Publikationen von Vázquez-Rowe et al. (2015) und Golkowska et al. (2015) zu finden.

Die gewichteten Ergebnisse, die den Schwerpunkt auf menschliche Gesundheit und Klimawandel legen, zeigen, dass die Behandlung von Gärresten und anschließendes Ausbringen auf die Felder weniger Umweltauswirkungen verursacht als direktes Ausbringen der Gärreste (siehe Abbildung 2). Die größte Reduktion der Umweltauswirkungen lässt sich durch die Behandlung von Rohgärresten (C, D) erzielen. Insgesamt wurden die zusätzlichen Umweltauswirkungen, die durch die teils aufwendige Aufarbeitung der Gärreste entstehen und mit dem verstärkten Energie-, Materialien- und Mineralienverbrauch verbunden sind, hauptsächlich durch bedeutende Reduktionen von Ammoniakemissionen kompensiert, welche sich in der Schadenskategorie „Partikelbildung" (PB) niederschlagen. Eine Ausnahme hierzu stellt das Kompostierungsszenario (A) dar, in dem kein großer Unterschied zwischen Behandlung und Direktausbringen zu sehen ist. Aus dieser Hinsicht ist die Kompostierung von stapelbaren Gärresten nicht zu empfehlen, da die zusätzlichen Behandlungskosten durch keinen entsprechenden Umweltnutzen kompensiert werden.

Durch die Wichtung der Ergebnisse bei der Berechnung von Sammelindikatoren, können die mit dem Ökosystem verbundenen Umweltauswirkungen unterrepräsentiert werden. In diesem Zusammenhang zeigt es sich, das besonders das Ammoniak-Strippen und Trocknen (C) aber auch Trocknen und Pelletieren (B) ein viel stärkeres Toxizitäts- und Eutrophierungspotenzial als die entsprechenden Vergleichsszenarien (BAS-2 und BAS-3) aufweisen. Die Erhöhung von Transportdistanz für die Endprodukte um 50% (von angenommenen 250km auf 500km) übte keinen großen Einfluss auf die Analysenergebnissen aus, während Nutzung von alternativen Ausbringungsverfahren für die Behandlungsprodukte (Flächeneinarbeiten, Bodeninjektionen) nur im Falle von Anlagen, die Rohgärrest behandeln, zusätzliche Umweltgewinne verschafft. Andererseits kann die Differenzierung von Versorgungsquellen für Strom und Wärme, zur deutlichen Reduzierungen der Umweltimpakte beitragen.

Ist Gärrestbehandlung ökonomisch tragbar?

Die durchgeführte Wirtschaftlichkeitsanalyse berücksichtigte die Gesamtinvestitionskosten (Gebäuden, Installationen, Infrastruktur, Maschinen, Landbeschaffung), Betriebskosten (Strom und Wärme, Materialien, Chemikalien, betriebsinterner Transport, Betriebskosten für die Installationen), sowie Personalkosten (Mitarbeiter), exklusive Mehrwertsteuer. Jede Anlage wurde für 20 Jahre kalkuliert und es wurde keine Form von finanzieller Unterstützung in der Analyse miteingerechnet. Die Kosten des Transports der Gärreste zur Behandlungsanlage wurden ebenfalls nicht einbegriffen. Ein Direktvergleich der unterschiedlichen Behandlungssysteme war nicht möglich, da jede Anlage insbesondere im Hinblick auf ihre Energieversorgung sehr unterschiedlich ist und verschiedene Energieträger (Biogas, Erdgas, Mischszenarien, etc.) nutzt. Um die Analyse möglichst transparent und übertragbar auf andere Länder/Regionen zu machen, wurde angenommen, dass der Gesamtenergiebedarf (Strom und Wärme) durch den Energieeinkauf gemäß aktuellem Marktpreis gedeckt wird. Weitere Informationen bezüglich der Studie sind dem Artikel Golkowska et al. (2014) und dem Bericht von Golkowska et al. (2015) zu entnehmen.

Die kalkulierten Behandlungskosten wurden auf das Eingangs- und Ausgangsvolumen bezogen, um einerseits die Kosten zwischen verschiedenen Behandlungssystemen vergleichen zu können, aber andererseits auch das Verhältnis zu den Marktpreisen der Produkte darzustellen. Die Ergebnisse der Auswertung sind in der Tabelle 1 zusammengefasst. Beim Vergleich von Behandlungskosten für verschiedene Anlagen (Tabelle 1) wird klar, dass, bezogen auf das Eingangsvolumen, die Behandlung via Kompostierung (A) (6€/Tonne Input) ökonomisch gesehen allen anderen Behandlungsmethoden überlegen ist. Deutlich darüber liegen die Behandlungskosten der aufwendigeren Methoden: für die Trocknungsanlage B (14€/Tonne Input) liegen die Kosten nur um 2€/Tonne input niedriger, als für die Umkehrosmose, biologische Behandlung und Trocknung der Anlage D (16€/Tonne Input). Dabei ist zu beachten, dass der Input der Anlage D (rohes Gärrest mit Trockensubstanzgehalt von 9-11% in der Frischmasse), mit dem der Anlagen A und B (vorbehandelter Gärrest mit Trockensubstanzgehalt von 26-55% in der Frischmasse) nicht vergleichbar ist und ganz andere Eigenschaften aufweist. Die Vorbehandlungskosten sind nicht bekannt und wurden somit nicht in die Analyse integriert. Die Anlage C wurde aus der ökonomischen Sicht nicht analysiert, da es sich dabei und ein theoretisches Szenario handelt.

Da die Anlagen A und B das stapelbare Substrat mit hohem Trockensubstanzgehalt behandeln, fällt die durch die Behandlung verursachte Volumenreduktion viel kleiner aus, als für die Anlagen C und E, die rohen Gärrest behandeln. Infolgedessen, unterscheiden sich die Input- und Output-bezogenen Kosten für die Anlagen A und B nur gering, während für die Anlagen C und E der Unterschied deutlich größer ausfällt.

Regionaler Mehrwert gegenüber interregionalen Geldflüssen

Die Behandlungskosten, die während der ganzen Lebenszeit der Anlage entstehen, sind zwei Kategorien zuzuordnen: regional verbleibende Geldflüsse (Kosten die zur Entwicklung der Region beitragen) und exportierte Geldflüsse (verbunden mit dem Geldfluss aus der Region). Der größte Teil der Kosten

		Kompost + $(NH_4)_2SO_4$ Lösung (A)	Getrockneter Gärrest + $(NH_4)_2SO_4$ Lösung (B)	Konzentrat aus Umkehrosmose + Getrockneter Gärrest (D)
Behandlungskosten	€/t Input	5.8	14.0	16.0
	€/t Output	8.0	19.0	246.9
Potenzieller Dünge- und Humuswert (PDHW)	€/t Output	21.3 (43.4)*	56.5	51.4

*21.3€ berücksichtigt nur die im kompostierten Gärrest enthaltenen Nährstoffe, während sich der Preis von 43.4€ auf die allgemeine Kompostcharakteristik bezieht, da der Kompost in dieser Anlage aus verschiedenen Biomassenströmen hergestellt wird

3_ Behandlungskosten und potenzieller Dünge- und Humuswert verschiedener Behandlungsprodukte (Golkowska et al., 2014 & 2015)

jeder Anlage ist mit der Energiebeschaffung (23-37%) und personellen Kosten (29-37%) verbunden, während die Investitionskosten 14-26% den Gesamtkosten ausmachen. Demzufolge kann die Nutzung lokal erzeugter Energie (z.B. aus Biogas) einen starken positiven Einfluss auf die lokalen Geldflüsse haben. Generell stärken die Nutzung lokal erzeugter Energie und die Einbindung lokaler Unternehmen in die Bau- und Planungsphase den regionalen Geldfluss und können dessen Anteil auf 75-93% der Gesamtkosten aufstocken. Das ist eine wichtige Information für Investoren und Entscheidungsträger, die durch Ihre Entscheidungen einen enormen Einfluss auf die regionale Entwicklung haben können.

Düngewert gegenüber aktuellem Marktpreis

Der potenzielle Dünge- und Humuswert (PDHW) für die Gärrestbehandlungsprodukte wurde auf der Basis der für die Pflanzen direkt verfügbaren N, P_2O_5, K_2O und Humus-C Mengen erstellt.
Die Kalkulation berücksichtigte die aktuellen Marktpreise für diese Nährstoffe. Die PDHW für die 4 analysierten Behandlungssysteme zusammen mit den Input- und Output bezogenen Behandlungskosten sind in Tabelle 1 zusammengefasst. Dieser Vergleich zeigt, dass wenn die Produkte der Anlagen A und B (die stapelbare Gärreste behandeln) einen Verkaufserlös in Höhe des halben PDHW erreichen würden, die Behandlungskosten komplett von den Verkaufsgewinnen gedeckt werden könnten. Für die Produkte der Anlage D gäbe es weiterhin Kosten in der Höhe von 12.6€/Tonne Input, auch wenn der Verkaufspreis den maximalen PDHW erzielen würde. Diese Kosten müssten entweder vom Gärrestlieferanten oder durch irgendeine Form von finanzieller Unterstützung gedeckt werden. In keiner der analysierten Szenarien sind die externen Transportkosten (ca. 8.50€/Tonne und 100km) inbegriffen. Diese Kosten müssen entweder vom Endnutzer gedeckt werden oder als Zusatzkosten in die Behandlungskosten miteinfließen, was im Falle der Anlagen B und D entweder höhere Abgabekosten für die Gärrestlieferanten oder gesteigerten Bedarf an finanzieller Unterstützung bedeutet.
Wenn man die aktuelle Rechtslage und Marktsituation von Gärresten und deren Behandlungsprodukten in Europa analysiert, wird es deutlich, dass der PDHW nur als hochtheoretischer Verkaufspreis von behandelten Gärresten betrachtet werden kann. In Wirklichkeit, hängen die Preise der Gärrestprodukte nicht nur von deren Qualität, sondern auch vom Einsatzbereich (z.B. Landwirtschaft, Gartenbau, Landschaftsgärtnerei, Hobbygartenbau), den hergestellten Mengen oder dem geographischem Standort ab (Barth, 2006; Kellner et al. 2011). Viele Gärrestbehandlungsanlagen sind gezwungen ihre Produkte kostenlos abzugeben. Manche schaffen es die Produkte für 2-10€/Tonne zu verkaufen, während die Anderen die Produkte über längere Distanzen transportieren um dabei bis zu 30€/Tonne (inklusive aktuellen Transportkosten von 8.50€/Tonne und 100km) erzielen zu können.

Erkenntnisse der Studie

Aus der ökonomischen und ökologischen Sicht ist es immer am sinnvollsten, wenn möglich, an erster Stelle die Überschüsse an Gärresten durch Extensivierung der lokalen Landwirtschaft zu vermeiden. Sollte dies nicht möglich sein, dann kann die Behandlung von Gärresten aus der Umweltperspektive klare Gewinne bringen, besonders wenn der Rohgärrest behandelt wird. Andererseits lässt sich, aus der ökonomischen Sicht, die Behandlung allein durch die Einkünfte aus dem Produktverkauf nicht finanzieren. Auch wenn die in den Produkten enthaltenen Nährstoffe ihrem Marktpreis entsprechend vergütet würden, wäre dies im Falle komplexer Aufbereitungstechnologien und der Behandlung von Rohgärrest nicht kostendeckend.
Demzufolge, in den Regionen in denen Gärrestbehandlung als Ausweg aus dem Nährstoffüberschuss angestrebt wird, müssen alternative Finanzierungsmöglichkeiten zur Deckung der Behandlungskosten gefunden werden, sei es durch Gärrestabgabegebühren oder andere Formen finanzieller Unterstützung, die die ökonomische Stabilität der Behandlungsanlagen garantieren können. Wichtig bleibt es dabei die Anlagen so zu konzipieren, dass der größtmögliche Geldfluss in der Region verbleibt und zu deren Weiterentwicklung beiträgt.

Danksagung

Die Autoren danken Ian Vázquez-Rowe (ehemals CRP Henri Tudor , heute La Pontificia Universidad Católica del Perú) für die Ökobilanzierung, und den Flämischen Projektpartnern – Viooltje Lebuf von VCM, Erick Meers, Evi Michels und Céline Vaneeckhaute der Universität Ghent, sowie Bart Ryckaert von Inagro für die Daten und den Knowhow-Transfer.

www.list.lu

Referenzen:

BMU, (2009): Characteristics of renewable energies, numbers and values. Berlin, Germany. http://www.umweltnundesamt-daten-zur-umwelt.de.

C. Fabbri, M. Soldano, S. Piccinini, (2010): The farmer believes in biogas and the number bears this out. In: Informatore Agrario, 66(30), 63-67.

EUROBSERV'ER, (2008) : Baromètre Biogaz. Systèmes Solaires, le journal des énergies renouvelables, 186, 45-59, (http://www.eurobserv-er.org/pdf/baro186_a.pdf), [in French].

EUROBSERV'ER, (2010) : Baromètre Biogaz. Systèmes Solaires, le journal des énergies renouvelables, 200, 105-119, (http://www.eurobserv-er.org/pdf/baro200b.pdf), [in French].

T. Prapaspongsa, P. Christensen, J. H. Schmidt, M. Thrane, (2010): LCA of comprehensive pig manure management incorporating integrated technology systems. In: Journal of Cleaner Production, 18(14) 1413-1422.

T. Rehl, J. Müller, (2011): Life cycle assessment of biogas digestate processing technologies. In: Resources, Conservation and Recycling, 56(1), 92-104.

F. Brouwer, P. Hellegers, M. Hoogeveen, H. Luesink, (1999): Managing nitrogen pollution from intensive livestock production in the EU. Agricultural Economics Research Institute (LEI), the Hague, pp. 23-42.

V. Lebuf, F. Accoe, C. Vaneeckhaute, E. Meers, E. Michels, G. Ghekiere, (2012): Nutrient recovery from digestates: techniques and end-products. In: Proceedings of the Fourth International Symposium on Energy from Biogas and Waste, Venice 2012.

J. B. Holm-Nielsen, T. Al Seadi, P. Oleskowicz-Popiel, (2009): The future of anaerobic digestion and biogas utilization. In: Bioresource Technology, 100(22), 5478-5484.

K. Golkowska, I. Vázquez-Rowe, E. Benetto, D. Koster, (2012): Life cycle assessment of ammonia stripping treatment of biogas digestate. 4th International Symposium on Energy from Biomass and Waste, Venice 2012.

I. Vázquez-Rowe, K. Golkowska, V. Lebuf, F. Accoe, E. Benetto, D. Koster, (2013): To treat or not to treat? Environmental assessment of digestate drying technologies using LCA methodology. 13th World Congress on Anaerobic Digestion. Recovering (bio) Resources for the World. Santiago de Compostela, Spain. June 2013.

P. E. Fixen, A. M. Johnston, (2012): World fertilizer nutrient reserves: a view to the future. In: Journal of the Science of Food and Agriculture, 92(5), 1001-1005.

I. Vázquez-Rowe, K. Golkowska, V. Lebuf, C. Vaneeckhaute, E. Michels, E. Meers, E. Benetto, D. Koster, (2015): Environmental assessment of digestate treatment technologies using LCA methodology. In: Waste Management, submitted.

K. Golkowska, I. Vázquez-Rowe, V. Lebuf, C. Vaneeckhaute, E. Michels, E. Meers, E. Benetto, D. Koster (2015): Life Cycle Assessments of selected processes of nutrient recovery from digestate. In: E. Meers & G. Velthof, eds. The recovery and use of mineral nutrients from organic residues, Wiley, in preparation."

K. Golkowska, I. Vázquez-Rowe, V. Lebuf, F.Accoe, D. Koster (2014): Assessing the treatment costs and the fertilizing value of the output products in digestate treatment systems. In: Water Science and Technology, 69(3), 656-662.

J. Barth, (2006): Quality and markets for compost and digestion residues in Europe. The 1st Baltic Biowaste Conference, Tallinn, Estonia, www.recestonia.ee/ecn/presentations/9%20Josef%20Barth.pdf (accessed 03 June 2012)

U. Kellner, R. Delzeit, J. Thiering, (2011): Digestate treatment: The influence of the location and size of the plant on the cost. Berichte über Landwirtschaft, 89(1), 38-55.

It is now well known that the quality of electric power is a key factor for the electricity service. It defines how good the characteristics (amplitude and frequency) of the supplied power meet the rated ones. Voltage dip (or sag) and swell, short and long interruptions, voltage spike, under and over voltage, harmonic distortion, voltage unbalance are the common power quality problems. Among these last, the harmonics issue is getting more and more important over the last decades and this trend will surely continue its race. This is essentially due to the widespread use of electronic components in electric equipment: it changes the nature of the electric loads from linear to non-linear and makes them, on the one hand, responsible for the harmonics generation in the power grid but very sensitive to the power quality problems on the other hand.

uni.lu
UNIVERSITÉ DU LUXEMBOURG

DISTRIBUTED HARMONIC COMPENSATION FOR POWER QUALITY IN SMART GRIDS_

Patrick Kobou Ngani, Prof. Dr.-Ing. Jean-Régis Hadji-Minaglou, Prof. Dr.-Ing. Emmanuel De Jaeger, Prof. Dr.-Ing. Michel Marso

What are harmonics?

Harmonics are voltages or currents waves of which the frequencies are integer multiples of the fundamental frequency; this means, for a grid with the fundamental frequency of 50 Hz, the fifth and seventh harmonic frequencies would be 250Hz and 350Hz respectively. A harmonic distorted waveform will no longer be a pure sine wave. It is important to mention that harmonics are generally considered as a steady state phenomenon and therefore not to be confused with spikes, dips and other forms of transient events.

Causes and effects of harmonics

As mentioned before, harmonics are produced by non-linear loads that draw non-sinusoidal currents. Their main characteristic is actually that the waveforms of the drawn current is not purely sinusoidal, even if they are fed by a perfect sinusoidal voltage. A distinction can be made between two groups of non-linear loads: The "modern" non-linear loads including energy converters based on power electronic components and the "classical" non-linear loads not related to the power electronics but, for instance, to:

_Transformers
_Rotating machines
_Fluorescent lamps with magnetic ballasts
_Arc furnaces
_Welding machines

Already in use for many decades, these loads rely on the magnetization effect where they operate near the knee of the saturation curve of the material (of which the magnetic characteristic is not linear). There are also arcing devices; their operating voltage-current characteristics are extremely non-linear.

"Modern" non-linear load are for example:

_Inverter fed AC voltage sources
_Adjustable speed drives (ASD)
_Energy-efficient lighting
_DC converters

These appliances are based on semiconductors devices like diodes, IGBT's, GTO's. The different generated harmonics (frequency and amplitude) depend on the topology, design and operating principle of the switching circuits. For example, a 6-pulse rectifier will cause harmonic at the 5th, 7th, 11th, 13th, etc. order. In this case, the amplitude of each harmonic is estimated to be inversely proportional to the harmonic order). The one generated by the 12 pulse rectifier are the 11th, 13th, 23th, 25th, etc. with amplitudes of about 10 percent of those for the 6-pulse rectifier [1]. Generally, line-commutated devices (such as the ones mentioned before) will also have harmonic characteristics different from those of forced commutation devices (such as PWM converters)

The major effects generated by the harmonics are resonance, increase of RMS voltage and current values and excessive neutral currents [2]. These may have as direct consequences:

_Overheating of equipment and grid components,
_Malfunction of circuit breaker,
_Capacitor damage,
_Malfunction or damage of sensitive electronic equipment,
_Motor shaft torque perturbation,
_Equipment lifetime shortening,
_Noise in communication signals.

On a second level, once an equipment is damaged, part of the whole power supply can be interrupted and most of the time it's only at this stage that the harmonics distortion problem is visible.

The economic impact due to these material-related effects, which can lead to power outages, is very big. The digital economy (data storage, retrieval and processing), the continuous process manufacturing (paper, oil, clay, steel, glass) and the fabrication and essential services (railroads, wastewater treatment) are the three sectors most sensitive to the power quality problems [3].

In the USA, they are collectively losing 6.7 billion dollars every year due to the power quality disturbances [3]. A survey realized by the Electric Power Research institute (EPRI) reveals that the harmonics are the source of 22% of all the power disturbances [4].

Harmonics mitigation technics

Many solutions have been developed to overcome the problem of the harmonic pollution [2] [5] [6]:

_Passive power filters (PPF): They are based on combining passive electrical components like inductances and capacitors to obtain a specific resonance frequency that counteracts a chosen harmonic frequency. Due to their proven efficacy and low cost, they are widely used in

industry. Because they are built up from specific elements they are hardly adaptable and the combination of more passive filters creates a resonance phenomenon between the filters that can cause the destruction of the filters elements.

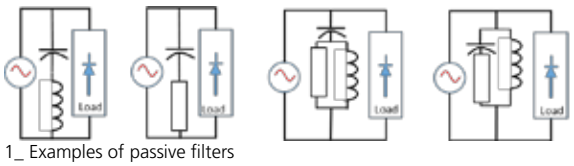

1_ Examples of passive filters

_Active power filters (APF): Based on controlled power inverters working as current or voltage sources, they create, in parallel (shunt APF) or in series (Series APF), harmonic currents or voltages in the power grid that are in opposition to the existing harmonics. The main advantages for APFs compared to PPFs is their better harmonics attenuation efficacy and their adaptability to the system changes (harmonic amplitude and frequency). They are also able to compensate more than one harmonic order without leading to the resonance problem. In contrast the use of power electronics (Semiconductors, current and voltages sensors, microcontroller) makes them quite expensive and the high switching frequency creates HF disturbances and noise that also needs to be eliminated through additional filtering.

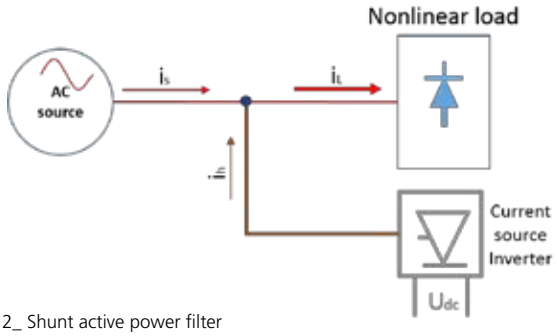

2_ Shunt active power filter

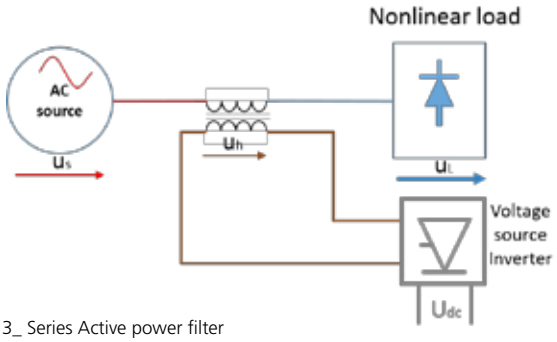

3_ Series Active power filter

_Hybrids power filters: They benefit of the advantages of PPFs and APFs with improved performance and cost-effective solution. The harmonic mitigation task is shared between the APF and the PPF. The most common task distribution is to let the APF filtering the harmonics of lower frequency, while the PPF filters the high frequencies harmonics.

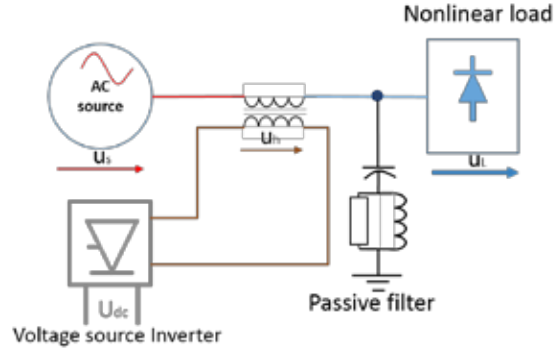

4_ Hybrid series active filter

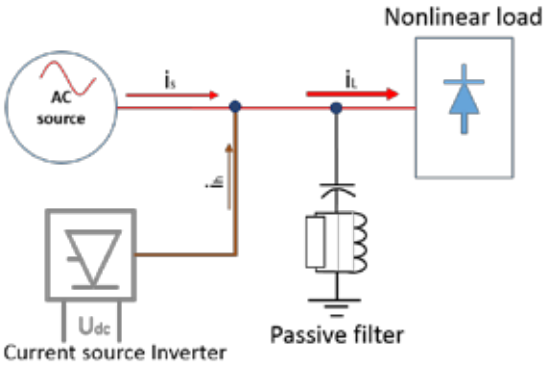

5_ Hybrid shunt active filter

The project at the University of Luxembourg

An original active power filter concept is now under development in the Research Unit in Engineering Science of the University of Luxembourg. The filter helps the supply voltage of the grid it is connected to, to meet the harmonics requirements defined by the European standard on the electric power quality EN50160. The developed APF is therefore a voltage harmonics filter because the standard focuses only on the utility grid voltage; guidelines for current waveform characteristics being almost impossible to realize due to the individual intrinsic functional behaviour of each electric equipment.

Figure 6 presents the drive (in an electrical cabinet shape), as a conventional active power filter with the selective harmonics detection and compensation ability of the filter. Synchronized to an existing power grid that supplies a non-linear load, the filter is a pure power conditioning element: it generates and injects into the grid the inverse of the harmonics generated by the load so that the resulting waveform has a lower harmonic distortion (due to those not compensated by the filter).

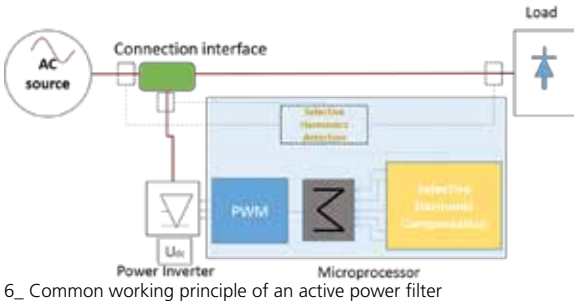

6_ Common working principle of an active power filter

The system, besides the ability to work as a conventional APF, has dedicated specifications that make it work as:

_An auto-compensated power voltage source or backup power supply:
In an off-grid situation, electrically fed by any renewable energy source (photovoltaic, wind or hydro turbine), the filter does not only provide the rated power system voltage and frequency (230V and 50Hz) but also removes the possible harmonics that might have been caused by any non-linear load connected on the local grid. The inverter generates an output voltage being a distorted waveform so that, combined with the harmonic distortion created by the non-linear load, the resulting waveform tends to a pure sine wave.

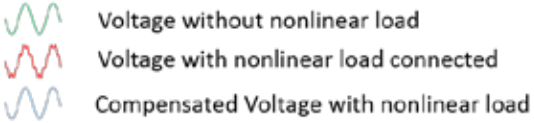

7_ Power inverter as voltage source with harmonics compensators

_A part of an harmonics compensators network:
Having the feature of a selective compensation, one can figure out a global compensation work done by a number of interconnected filters connected on the same power grid. For example, tied on the same grid and having

different renewable power sources available, two filters could cooperate to improve the power quality. The first will mitigate only 50% of the 5th harmonics and the second, with more power available, will removes the other 50% of the 5th, 100% of the 7th and only 20% of the 11th harmonic.

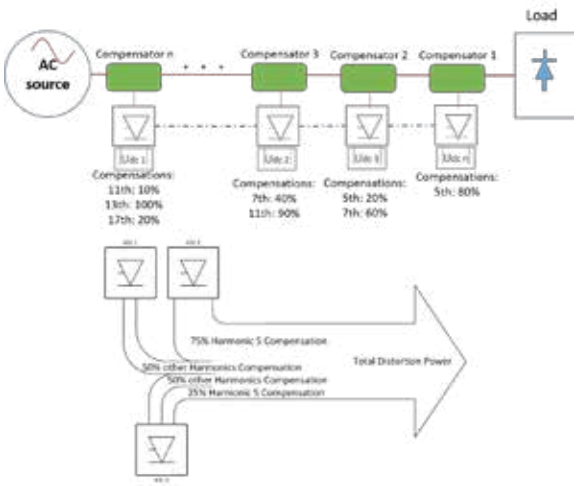

8_ Interconnected APFs (top) for a distributed harmonics compensation (bottom)

Figure 9 illustrates the actual state of the test rig used for the fulfilment of the project. The central element is the microprocessor: the CompactRio realtime microcontroller of National Instrument (NI). It's a reconfigurable, embedded, modular acquisition and control system that includes a reconfigurable FPGA chassis and a real-time controller programmable in the NI LabVIEW programming language. The grid-fed DC voltage source is used to simulate the power supply from renewable sources. The power inverter, fed by the DC voltage source, is a 15 kHz IGBT-based inverter. The passive power filter is used to eliminate the high switching frequencies of the inverter from 4 kHz on, i.e. there is no low-frequency harmonics mitigation by this filter; neither the ones created by the load nor the compensation's frequencies generated by the inverter.

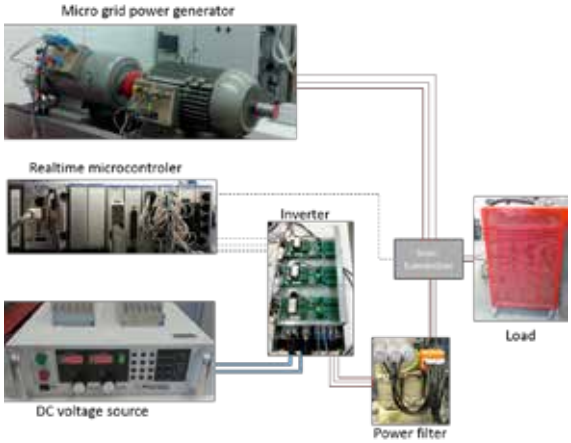

9_ Current test rig at the University of Luxembourg

A MATLAB simulation with concluding results has already been done for a resistive non-linear load. The simulated model will be extended to the most realistic resistive-inductive and capacitive load. Meanwhile, the implementation of the core elements on the test rig for real-time operation has started: Sensors data acquisition, voltage source inverter command by a pulse width modulation (PWM), numeric filters. Different compensation methods (algorithms) will be tested to determine, according to different goals (compensation dynamic, efficacy, adaptability to load changes), which one is the most appropriate.

This project contributes to the evaluation of the technologic, energetic and economic costs of the harmonics compensation with respect to the current quality standards, taking into consideration the evolution of the power generation systems trending to low power distributed units as well as the consumption systems made of numerous and multiple small electronic devices (TV's, smartphones, computers, teeth brushes etc.).

Abbreviations

APF:	Active Power Filter
CSI:	Current Source Inverter
PPF:	Passive Power Filter
PWM:	Pulse Width Modulation
VSI:	Voltage Source Inverter

www.uni.lu

References

1_R. G. Ellis, „POWER SYSTEM HARMONICS. A Reference Guide to Causes, Effects and Corrective Measures," Rockwell Automation, 2001.

2_C. Surajit, M. Madhuchhanda und S. Samarjit, Electric power Quality, Springer, 2011.

3_David Lineweber und Shawn McNulty, „The Cost of Power Disturbances to Industrial & Digital Economy Companies," Primen, 2001.

4_Sharmistha Bhattacharyya and Sjef Cobben, „Consequences of Poor Power Quality – An Overview," In Tech, 2011.

5_Zainal Salam, Tan Perng Cheng und Awang Jusoh, „Harmonics Mitigation Using Active Power Filter: A Technological Review," Elektrika, Bd. 8, Nr. 2, pp. 17-26, 2006.

6_Hirofumi Akagi, „New Trends in Active Filters for Power Conditioning," IEEE Transactions on Industry Applications, Bd. 32, Nr. 6, pp. 1312 - 1322, 1996.

La capture et le stockage du CO2 est considéré comme une alternative prometteuse pour atteindre les objectifs de réduction des émissions de carbone de la production d'électricité. En développant et appliquant une stratégie d'optimisation thermo-environomique, le bénéfice environnemental et les coûts énergétiques et économiques sont évalués de manière systématique pour différentes options technologiques de la capture du CO2.

LE COÛT DE LA CAPTURE DE CO2 DANS LES CENTRALES ÉLECTRIQUES_

Dr. Laurence Tock

Face aux enjeux de la réduction des émissions de gaz à effet de serre (GES) et de l'approvisionnement durable en énergie, la capture et le stockage du CO2 (CCS, «Carbon capture and storage») est l'une des mesures clés qui pourrait contribuer à l'objectif de réduire les émissions de GES de 20% jusqu'en 2020. Dans la perspective du tournant énergétique s'annonçant en Europe, la capture et la séquestration du CO2 dans la production d'électricité fait partie des mesures requises.

Pour évaluer la compétitivité du CCS et apporter une aide à la prise de décision, une approche systématique pour l'analyse et la conception de procédés a été développée et appliquée.

Capture et stockage du CO2

Le captage-stockage du CO2 se résume en trois étapes: la capture consistant en la séparation du CO2 du gaz résiduel; le transport par bateau ou gazoduc jusqu'au lieu de stockage (compression à 110 bar) et le stockage à long terme dans des formations géologiques (p.ex. réservoirs de pétrole ou de gaz épuisés, aquifères salins).

Pour l'étape de capture trois concepts différents peuvent être envisagés (Figure 1):

_La postcombustion séparant le CO2 des fumées (N2 et H2O) en aval de la combustion.

_L'oxycombustion utilisant l'oxygène pur, au lieu de l'air comme oxydant pour la combustion qui génère un gaz de combustion contenant de l'eau et du CO2 pouvant être séparé simplement par condensation de l'eau.

_La précombustion où le combustible est d'abord converti en gaz de synthèse (CO et H2) soit par reformage du gaz naturel, soit par gazéification de la biomasse ou du charbon.

Le gaz de synthèse réagit ensuite avec de l'eau par la réaction de shift (WGS) pour générer du CO2 et de l'hydrogène. Après séparation du CO2, l'H2 peut être brûlé dans une turbine ou être utilisé dans une pile à combustible pour produire de l'électricité.

Différentes technologies telles l'absorption chimique ou physique, l'adsorption ou les procédés membranaires peuvent être utilisées pour séparer le CO2. Outre leur maturité technologique, ces procédés se distinguent par leur taux de capture du CO2, leur consommation en énergie et par les coûts d'investissement.

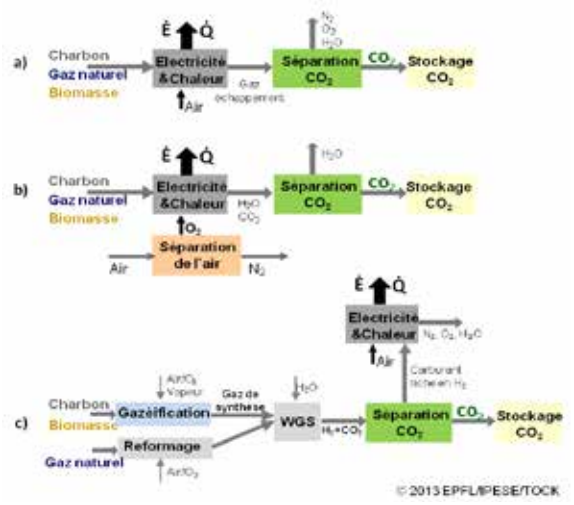

1_ Concepts de la capture de CO2: a) post-; b) oxy-; c) pré-combustion

Défis du CCS

Si le potentiel de réduire les émissions de CO2 dans la production d'électricité par CCS est important, le coût énergétique et économique représente un désavantage majeur. En moyenne, la capture du CO2 augmente la consommation d'énergie de 10% et les coûts d'investissement de près d'un tiers. Pénalisant les procédés classiques l'introduction d'une taxe sur le CO2 émis peut compenser ces désavantages en partie.

Il est donc important de disposer de méthodes systématiques qui permettent de comparer des options et de développer des procédés intégrant de manière optimale les techniques de capture du CO2 afin d'évaluer leur compétitivité thermo-environomique sur le marché.

Stratégie d'optimisation multi-objectf

Pour comparer les différentes options, le groupe «Industrial Process and Energy Systems Engineering» de l'EPFL a développé une méthode pour la conception, l'analyse et l'optimisation thermo-économique et environnementale de procédés. Cette méthode illustrée dans la Figure 2 combine la simulation de procédés avec les techniques d'intégration énergétique, l'évaluation des coûts, l'analyse du cycle de vie (ACV) et les techniques d'optimisation multi-objectif.

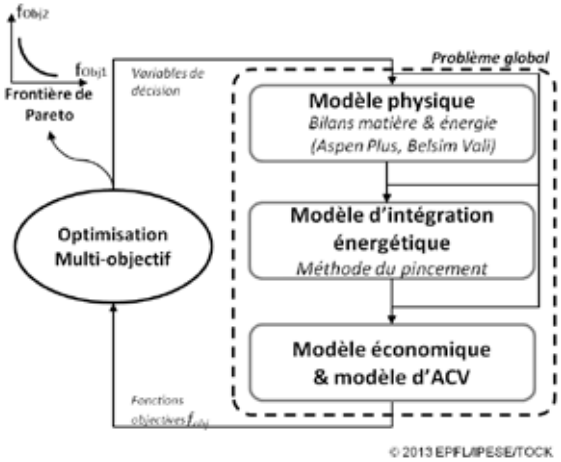

2_ Méthodologie d'optimisation thermo-environomique

Après avoir identifié les technologies potentielles, les transformations chimiques et physiques de chaque procédé sont simulées et les besoins énergétiques identifiés. Afin d'améliorer l'utilisation rationnelle de l'énergie, la récupération de chaleur dans le procédé est maximisée et l'efficacité de la conversion des ressources est optimisée en appliquant des techniques d'intégration énergétique, comme la méthode du pincement.

À partir de ce résultat, chaque équipement du procédé est dimensionné. Les coûts et impacts environnementaux sont ensuite estimés sur la base de la taille.

La compétitivité est évaluée par les indicateurs de performance suivants:

_L'efficacité énergétique ε, est définie par le ratio entre la quantité nette d'électricité produite et la quantité d'énergie entrant dans le système sous forme de combustible (basée sur le pouvoir calorifique inférieur).

_Le prix de revient comprenant le coût d'investissement annualisé, les coûts opératoires, les coûts de maintenance et les taxes éventuelles. Un taux de change de 1,2 CHF/€ a été considéré.

_Le taux de capture du CO2 représente le ratio molaire entre le carbone capturé et celui entrant avec le combustible.

_L'impact environnemental calculé par l'ACV prend en compte les impacts de l'extraction des ressources jusqu'au produit final.

Le choix des technologies et les conditions opératoires optimales sont ensuite définis sur la base de ces indicateurs en générant la frontière de Pareto qui représente le compromis idéal entre les objectifs tels que coûts et efficacité.

Pour résoudre le problème d'optimisation multi-objectif un algorithme évolutif est appliqué.

Compétitivité de la capture de CO2

Les configurations qui ont été étudiées sont; la capture de CO2 par post-combustion basée sur l'absorption chimique avec des amines dans une centrale à cycle combiné alimenté au gaz naturel et la capture de CO2 par pré-combustion basée sur l'absorption physique (Selexol) dans des centrales à gaz naturel (GN) et à biomasse (BM).

Le stockage du CO2 n'est pas pris en compte; seules la capture et la compression du CO2 à 110 bar pour le transport sont intégrées.

Compromis coût-efficacité

Les résultats de l'optimisation multi-objectif maximisant le taux de capture et l'efficacité énergétique pour différents scénarios économiques (Figure 3) mettent en avant le compromis entre l'efficacité, les coûts et l'impact environnemental.

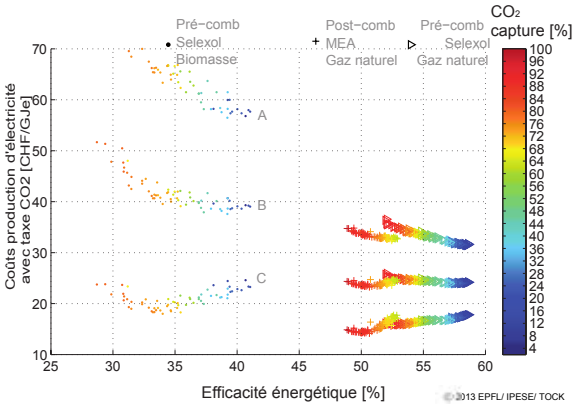

3_ Résultats de l'optimisation multi-objectif pour différents scénarios économiques.
Prix ressource- taxe carbone- heures d'opération - durée de vie- taux d'intérêts
A) 11.8€/GJe-16,7€/tCO2-4500h/y-15y-4%
B)8€/GJe-29€/tCO2 -7500h/y- 25y -6%
C) 4,5€/GJe-45€/tCO2 -8200h/y -30y-8%.

Il est à noter que ces résultats dépendent fortement de plusieurs facteurs tels que la maturité de la technologie (i.e. investissement), le coût du combustible, le montant de la taxe carbone, le temps d'opération, la durée de vie escomptée des installations et le taux d'intérêt. Les performances d'une centrale au gaz naturel avec 90% de capture et d'une centrale à biomasse avec 60% de capture sont comparées dans le Tableau I à une centrale conventionnelle à cycle combiné (CCGT).

Système	CCGT	Post-.	Pré-.	Pré-.
Capture	Pas CCS	MEA	Selexol	Selexol
Type ressource	Gaz nat.	Gaz nat.	Gaz nat.	Biomasse
Ressource [MW_{th}]	559	587	725	380
CO_2 capture [%]	0	89,5	89,1	59
ε [%]	58,7	49,6	**52,6**	34,8
Elec. nette [MW_e]	333	296	381	132
Emissions locales [$kg_{CO2,\ local}/GJ_e$]	105	14,9	11,5	**-170,4**
PRG [$kg_{CO2,\ eq}/GJ_e$]	120	34	31,9	**-134,2**
Invest. [€/kW_e]	462	757	677	3233
Prix revient [€/GJ_e][1]	15,2	**19,3**	20,4	41,2
Prix revient incl. taxe [€/GJ_e][1][2]	18,3 15,1-24	**19,7** **7,5.33**	20,7 10,6-35	30,2 12,5-58

4_Comparaison de la performance des procédés. 1Scénario B) 2_Variation entre les scénarios A) et C)

Pénalité énergétique

Par comparaison avec une centrale CCGT ayant un rendement de 58,7%, la pénalité de la capture du CO2 par précombustion correspond à 6% du pouvoir calorifique du combustible (PCI), alors que celle de la capture par postcombustion est de 9%. La perte énergétique est due à la consommation d'énergie pour la capture du CO2 et pour la compression du CO2 jusqu'à 110bar (environ 2% du PCI).

Dans un procédé avec capture du CO2, il est possible de valoriser la chaleur résiduelle du procédé de capture dans un chauffage urbain basse température (50 à 80°C) et ainsi de substituer l'utilisation du gaz naturel dans des chaudières. L'intégration du chauffage urbain diminue la pénalité de 9% à 1,2% pour la capture en postcombustion, rendant ainsi la solution de capture beaucoup plus efficace (57,6%). Ceci exige toutefois de placer la centrale électrique à proximité d'un chauffage urbain dont les besoins correspondent à 0,157kW thermique par kW d'électricité produite.

Considérant que les centrales à gaz seront principalement utilisées pendant la période de chauffage des bâtiments, soit un temps d'opération de 5000h/a, la chaleur mise à disposition pour le chauffage urbain par une centrale produisant 300MWe permettra de couvrir la consommation de 50000 habitants. L'efficacité plus faible de la production

d'électricité à partir de la biomasse (34,8%) s'explique par la difficulté de convertir un combustible solide et humide.

Impact environnemental

Le bénéfice environnemental de la capture du CO2 est exprimé en terme de potentiel de réchauffement global (PRG) calculé par le biais de l'analyse de cycle de vie (ACV) pour une unité fonctionnelle de 1GJe selon la méthode de calcul proposée par l'IPCC (Intergovernmental Panel on Climate Change) en 2007. Il correspond aux émissions équivalentes de CO2 incluant toutes les émissions de gaz à effet de serre depuis l'extraction de la ressource jusqu'au produit final. Les calculs d'optimisation permettent de déterminer un taux de capture optimal qui varie entre 84% et 90%, ce qui correspond à des émissions équivalentes de CO2 aux alentours de 34 kgCO2,eq/GJe contre 120 kgCO2,eq/GJe pour une centrale sans capture. Les centrales avec CCS utilisant la biomasse peuvent conduire à des émissions de cycle de vie négatives (-134 kgCO2,eq/GJe) à cause du caractère biogénique du carbone. La neutralité en matière d'émissions de carbone pourra être atteinte par un mixe électrique de centrales au gaz naturel (80%) et à la biomasse (20%).

Performance économique

La capture induit une augmentation du prix de revient de l'électricité de l'ordre de 20-25% (soit 1,7 à 2,1 cts/kWh) pour les cas utilisant comme ressource le gaz naturel (scénario B, figure 2). Comme les coûts de production d'électricité sont déterminés à 80% par le prix de la ressource, la réduction de la production d'électricité par capture du CO2 explique en grande partie cette augmentation. L'investissement augmente par rapport à une centrale sans capture CCGT de 46% pour la capture en postcombustion et de 68% pour la pré-combustion qui est plus complexe. Sur la base des résultats, la post- et la précombustion ne se distinguent pas clairement en termes de performance économique. Le procédé utilisant la biomasse résulte cependant en des coûts plus élevés à cause de l'investissement important lié à l'unité de gazéification et au coût d'achat de la biomasse. Ce procédé devient en raison de l'avantage environnemental prometteur si la biomasse est disponible à un prix bas et si la taxe carbone dépasse 52€/tCO2.

Compétitivité

La comparaison de la performance thermo-environomique des options de capture dans divers contextes économiques montre qu'en termes de réduction des émissions de CO2 le procédé utilisant la biomasse est le plus avantageux. Cependant, l'efficacité est plus faible et l'investissement plus élevé que pour la production d'électricité à partir du gaz naturel. Pour les centrales à gaz, la post- et la précombustion sont en compétition. La précombustion est légèrement plus efficace à cause de la qualité de l'intégration énergétique, alors que la postcombustion, qui a l'avantage d'être une solution de réaménagement (rétrofit), conduit à des coûts d'investissement plus faibles. En valorisant la chaleur résiduelle de la postcombustion pour le chauffage urbain, le prix de revient de l'électricité est très peu pénalisé et l'efficacité globale peut être augmentée à 57,6% et les émissions évitées seront de 885tCO2/an. Au final, ce sont le développement des technologies de CCS et le contexte économique qui détermineront la compétitivité sur le marché.

Conclusions

L'application d'une approche systématique pour la conception, la comparaison et l'optimisation de procédés, tenant en compte simultanément des aspects thermodynamiques, économiques et environnementaux, a permis de comparer et d'optimiser l'intégration des procédés de capture du CO2 dans les centrales électriques utilisant des ressources fossiles ou renouvelables.
Il s'avère que les diverses options de capture de CO2 dans des centrales électriques sont compétitives, même avec des centrales conventionnelles sans capture de CO2, lorsqu'une taxe carbone est introduite. Le choix de la configuration optimale est défini par le but de production et les priorités données aux différents critères thermo-environomiques. Selon le contexte économique la configuration optimale, notamment le taux de capture optimal et le choix de la ressource et de la technologie, sera différente.

Dans le contexte actuel du revirement énergétique les options de CCS devront être envisagées pour limiter les émissions de gaz à effet de serra à moyen terme avant de parvenir à un approvisionnement basé principalement sur des ressources renouvelables. Il sera notamment important de considérer l'intégration des centrales à gaz avec capture de CO2 avec le chauffage urbain afin de limiter les pénalités dues à la capture et d'envisager l'utilisation de centrales à biomasse qui permettent indirectement de capturer le CO2 de l'atmosphère.

laurence.tock@gmail.com

Références

L.Tock: Thermo-environomic optimisation of fuel decarbonisation alternative processes for hydrogen and power production. EPFL Thesis no 5655, 2013. Doi:10.5075/epfl-thesis-5655.

Photo: Remise du prix lors de la Conférence ESCAPE-24 à Budapest

La Fédération Européenne de Génie Chimique (EFCE) a récompensé la chercheuse Luxembourgeoise, Dr. Laurence TOCK avec le prix d'excellence en reconnaissance d'une thèse de doctorat exceptionnelle dans le domaine de l'ingénierie des procédés assistée par ordinateur intitulée 'Thermo-environomic optimisation of fuel decarbonisation alternative processes for hydrogen and power production' effectuée à l'École Polytechnique Fédérale de Lausanne (Suisse) sous la direction du Prof. Maréchal.

EFCE communiqué de presse

The debris generated during the construction, renovation, and demolition of buildings, roads, and bridges is called construction and demolition wastes (C&D waste). They include: concrete, wood, asphalt, gypsum, metals, bricks, glass, plastics, building components like doors, windows, and plumbing fixtures, trees, stumps, earth, and rock from clearing sites.

UNIVERSITÉ DU LUXEMBOURG

USE OF RECYCLED CONCRETE IN CONSTRUCTION IN LUXEMBOURG_

Professor Dr. Ing. en Génie Civil Danièle Waldmann -Diederich, Vishojit Bahadur Thapa

Construction and demolition waste constitutes a major portion of total waste production in the world, and most of it is used in landfills.
The re-use of concrete rubble collected from demolished structures is an important issue. After crushing and screening, there is the possibility of appropriately treating and reusing such waste as aggregate in new concrete, especially in lower level applications.
Different aspects of the topic beginning with a brief review of the European initiatives and definition in terms of C&D waste generated and recycled aggregates produced from C&D waste are given. Along with a brief overview of C&D waste, a summary of the situation in Luxembourg in use of recycled aggregate is discussed.
This writing concludes by identifying some of the major barriers in more use of recycled aggregate concrete, including lack of awareness, lack of knowledge, barriers of specifications/codes for reusing these aggregates in new concrete.

Circular economy
A circular economy is a system that is restorative or regenerative by intention and design. It replaces the 'end-of-life' concept with restoration, reuse and recycling. In the context of concrete, a circular system can be achieved by transforming waste to a new raw material. This brings a double benefit to environment: Waste is eliminated and waste as a resource is used in an efficient and sustainable way.

_Source: Towards the circular economy - Reports - World Economic Forum

Using natural resources and converting, transforming them into goods is one of the principal economy foundation of our and earlier generations. And of course it will be an essential part of the future wealth. However statistics show that the quantity of our current resource use is at such a rate that the facility of future generations and the developing countries to access to their appropriate share of decreasing resources are endangered.
Knowing this, it is clear that the conception of resource efficiency has gained huge significance in all over the world, especially in Europe.

Europe is dependent on the rest of the world for many resources, such as fuel and raw materials, which are part of products imported from outside the European Union.
Our dependence on oil, gas and coal makes consumers and businesses vulnerable to damaging and costly price fluctuation. Shortage of resources and unpredictable product prices brings instability to the European economy which threatens our economic security.
Therefore several strategies and campaigns like 'The Roadmap to a Resource Efficient Europe (COM (2011) 571) ', 'Europe 2020 Strategy' and others, have been launched by the European Union and its partner countries in order to diminish this dependency and to build a resource efficient Europe.
Statistics and trends show that in order to achieve these goals, the improvement of the European waste management has to be stimulated and promoted.
The major plan is to turn waste into a resource so that we get a circular economy. Therefore objectives and goals are set in European policies and legislation in order to improve waste management, stimulate improvement and innovation in recycling, limit the use of landfilling, and initiate change consumer behaviour.

CEMBUREAU - Cement, concrete & the circular economy

Construction and demolition waste
The European Commission has identified construction and demolition (C&D) waste as a priority stream because of the large quantities that are generated and the high potential for reuse and recycling enclosed in these materials.
More precisely, statistics show that there is application of the huge quantity of products made of concrete in the construction sector and that its properties make it the most consumed material worldwide and the second most

consumed resource worldwide. So concrete has the highest potential to be recycled.
Generally, recycling concrete means reusing or recycling of demolished concrete for the purpose to use it as a secondary raw material for different fields of application: road construction, foundation, substructure, structural concrete, etc.
Recycled concrete aggregate is basically produced in two stages: Firstly, crushing of demolished concrete, and secondly, filtering and removal of contaminations and unwanted by-products such as reinforcement, paper, wood, plastics and gypsum. Concrete made with such recycled concrete aggregate is called recycled aggregate concrete.

In general, in Europe, when we speak about recycling of concrete, we speak about downcycling because a pure recycling of concrete for higher class raw material is economically unviable at the moment.

Down cycling describes the process of converting waste materials or useless products into a new, lower-value material or product. Downcycling aims to reduce waste and the consumption of new raw materials, energy usage, air pollution and water pollution.

Vishojit B. Thapa - RECYMA S.A. - C&D Waste

Situation in Luxembourg
The current situation of waste management considering concrete recycling and its application in Luxembourg is simple to scrutinize.
In comparison with the European average, Luxembourg generates the second highest share of the EU-28 considering mass per habitant. The high ranking is due to the high percentage of excavation material, like soils and rocks, which is included in the definition of C&D waste. This is largely responsible for the high amount of waste generated in Luxembourg.

For example, in 2010, the numbers about Luxembourg consolidates the overall European tendency, 8.6 million tons out of 10.4 million tons of total waste, was generated by the construction sector as construction and demolition waste.

From the total amount of eliminated and recycled inert waste in Luxemburg (2010):

_Inert waste
Consists of:
Eliminated inert waste (landfilling, earth and stone): 70%
Recycled inert waste: 30%
_From this recycled inert waste: 30%
Consists of:
Regional recycling centres: 21%
Other backfills: 1 %
Exported inert waste: 8 %

According to experts, among all the materials, concrete represents approximately 178 thousand tons (178 000 tons). This amount of tons is the quantity of recyclable concrete for 2010.
Additionally, experts estimate that currently in Luxembourg, for concrete waste, there is a high tendency of downcycling of concrete waste for use in road construction, foundation and substructure construction.
Luxembourg already fulfils by the requirement for concrete of the Waste Framework Directive which in general requires Member States to take any necessary measures to achieve a minimum target of 70 % (by weight) of construction and demolition waste by 2020 for preparation for reuse, recycling and material recovery, including operations using non-hazardous construction and demolition waste to substitute other materials.
The national network consists of 12 regional landfill sites exploiting inert waste. The quality of the recycled concrete aggregates generated in Luxembourg depends on several factors.
In Luxembourg, its origin is mainly from demolition of buildings, thus already the initial material is not pure concrete demolition and it has a considerable rate of contamination. Its minor constituents are bricks, tiles, ceramics, soils, gypsum, insulating material, timber, metals, etc. Considering these constraints, we can say that the recycled concrete in Luxembourg has an average quality.
In Luxembourg, there are two important documents which have to be consulted and followed while using recycled aggregates for concrete production:

_Combined document 'concrete', EN 206-1: Concrete - Specification, performance, production and conformity, completed by the national application DNA EN 206-1:2000

Original title: DOCUMENT COMBINÉ « BÉTON » constitué de la NORME EN 206-1: BETON, Partie 1: Spécification, performances, production et conformité, modifiée et complétée par le Document National d'Application luxembourgeois de l'EN 206-1: 2000

_Specification sheet: Aggregates

Original title: PONTS ET CHAUSSEES, CAHIER DES CHARGES: 'GRANULATS' (CDC-GRA08)

Additional to these national documents the following European Standard has high importance:

_EN 12620: Aggregates for concrete is most relevant for aggregates for structural concrete

According to these documents, the normal-weight aggregates have to be certified conforming to 'EN 12620: Aggregates for concrete' and the national specification sheet 'CDC-GRA Granulats et sables'.
The aggregates need a valid certification delivered by 'Laboratoire d'Essais des Matériaux des Ponts et Chaussées du Luxembourg' or need to be proved by the producer to have passed all the controls prescribed by the regulations in order to get a certification as aggregates and sand.

The recycled concrete aggregate have to submit a certification of adequacy delivered by an organisation approved in the framework of the directive 'Beton mit rezykliertem Zuschlag' from DAfStb (Deutscher Ausschuss für Stahlbetonbau; engl. German Committee for Structural Concrete).
In general, the following are the fields of application for recycled concrete aggregates in Luxembourg:

_Huge quantities are used in road constructions and foundation and substructure construction.
_Slight, minor quantities are used for the base or fill for drainage structures or piping systems. They are used to replace sand and gravel for the levelled assembly of extern piping of various systems.

As a conclusion, we can say that in Luxembourg recycled aggregates are mostly used in road construction and as sub-layer in foundation construction, but barely used in concrete production. In fact there are no statistics or accounting of its use as second raw material in concrete production in Luxembourg and it is difficult to find further information of their use in structural construction because this potential still hasn't gained ground in Luxembourg.
There are different reasons for this lack of use of recycled concrete aggregates for concrete production in Luxembourg. One important reason is the average quality of the recycled concrete aggregates, which makes the material unpredictable for concrete production.
As the material comes from construction sites, there is

always a certain degree of impurity of the material which changes from one construction site to another. This is also due to the strong scattering of the source material, which requires a separate and individual inspection

Furthermore, improved sorting and washing seems to be material-intensive and cost-intensive which leads to the inefficiency of the recycling process. There is a very low profit margin with the present processes. Besides, the limited quantities of material available in Luxembourg make it difficult to improve the processes and stimulate research in this field.
Finally, in the last centuries, Luxembourg's growth and wealth was driven by the steel industry and large reserves of blast-furnace slag, which are by-products from the steel production processes, had been made.
In the last decades, Luxembourg profited from these reserves for use in road and railway construction, but they are almost entirely spent. Therefore, the recycled concrete aggregates are used as slag replacement in road and foundation construction, drainage system, etc.


Workshop "Les bétons recyclés" - Chaux de Contern

Situation in neighbouring countries Belgium
In general, the situation in Belgium is slightly different from other countries. The geological context mainly influences the development of recycled concrete aggregates.

Belgium is divided in two main administrative regions which also represent two different geological regions, the Dutch-speaking region of Flanders in the north and the French-speaking southern region of Wallonia. The administrative region of Brussel plays a minor role on geological level.
In the region of Flanders, there are very low amounts of stone pits and quarries which explain its huge ambition in retrieval alternative aggregates accessible in short distances. So in general, the region of Flanders highly promotes the research and utilization of recycled concrete aggregates for numerous applications.
The region of Wallonia counts several sandstone quarries. This high occurrence of natural aggregates explains the high frequency of quarries in the southern regions. Additionally, the lobby of the quarries owner try to suppress the research and use of recycled aggregates to maintain their predominance and authority in the aggregates market. So, in the southern region there is the presence of a brake for the development of recycled aggregates.
Like it is general practice in the Greater Region, also in Belgium, the use of recycled aggregates is limited for application in sub foundations and road constructions. There are some construction projects consequently using recycled concrete in Belgium, but these are all individual and singular cases.

Germany
According to German experts, the utilisation of recycled concrete aggregates for recycled concrete production is possible and feasible, but in Germany there exist many restrictions.
Additionally, the stand of processes for recycled concrete is not efficiently practicable, therefore there is minor to no use in practice in Germany.
There are construction projects using only recycled concrete, but the number is very small comparing to overall construction projects and the motivation often comes from the environmental awareness of a small group of persons.
Additionally, high portions for the remote use of recycled concrete are the different additional requirements in German Standard which restrict the use of recycled concrete to very limited applications.

France
According to French experts, France has a slight backorder to other countries in the development of detailed and extensive procedures and requirements for the use of recycled concrete aggregates.
Therefore, the French government has launched a national project for research and development called RECYBETON. The aim of this project is to change the trend by re-using all the materials of deconstructed concrete, as components of new concrete or hydraulic binders, including the fine particles.

Summary
In general, valuable work has been done in several European countries in implementing research, development, pilot and demonstration projects, and in documenting best practice in fields such as selective demolition, the operation of recycling centres, and material-by-material processes.
The construction industry should therefore be encouraged to use alternative methods of managing material performance risks, including contract- or sector-specific specifications, or by the external verification of quality certification of recycled materials. It should not be necessary to wait for nationally or internationally agreed specifications.
Research plays a key role in deciding how quickly the sites are cleared and redeveloped, and this in turn strongly influences the extent to which selective demolition and the use of recycled concrete aggregates is practical.
Especially in Luxembourg, the awareness and importance about promoting new technologies and projects concerning recycling of concrete has not yet reached like, for example, in the neighbouring countries.
Luxembourg's government and construction companies have always been independent, efficient and sustainable in the aggregates and resource market. In the future, the competition and the well-known resource depletion will be more visible effects in the market. Therefore in Luxembourg, future plans and investments in recycling improvement have to take place on time.


Workshop "Rezyklierter Beton" - Université de la Grande Région

Acknowledgment
We would like to thank Mr. George Blasen from the 'Administration de l'environnement' for his expert advice and for sharing useful information and knowledge about concrete recycling in Luxembourg.
Additionally, we would like to thank the following construction companies for their cooperation and for taking their valuable time to show their recycling processes and providing some personal thoughts about concrete recycling in Luxembourg:

CLOOS - Bridel:	Tim Schlink, Director-General
Carrières FEIDT SA - Brouch:	Tom Rollinger, Site responsable
RECYMA - Hosingen:	Romain Coos, Director-General

References

1. European Commission - CONSTRUCTION AND DEMOLITION WASTE MANAGEMENT PRACTICES, AND THEIR ECONOMIC IMPACTS
Final Report - February 1999

2. European Commission - SERVICE CONTRACT ON MANAGEMENT OF CONSTRUCTION AND DEMOLITION WASTE – SR1
Final Report Task 2 - February 2011

3. Administration de l'Environnement - Aspects of modern waste management - collection of articles 2008

4. BIBM - The Concrete Case - Workshop on the Management of C&D waste in the EU

5. UEPG - A sustainable Aggregates Industry for a sustainable Europe

6. STATEC (Institut national de la statistique et des études économiques du Grand-Duché du Luxembourg)

7. European Commission - Eurostat

8. GRAND-DUCHE DE LUXEMBOURG - MINISTERE DES TRAVAUX PUBLICS
PONTS ET CHAUSSEES - CAHIER DES CHARGES

9. CEN: EUROPEAN COMMITTEE FOR STANDARDIZATION - European Standard

The PV-Forecast project will improve the forecasting performance of the photovoltaic (PV) electricity production for Luxembourg by using a combined approach of the monitoring of PV reference systems and the predictive modelling of the PV power based on meteorological weather prediction in order to increase the accuracy at higher spatial resolution.

PV-FORECAST: FORECASTING OF ELECTRICITY PRODUCTION FROM PHOTOVOLTAIC IN LUXEMBOURG_

Dipl. Ing. Frank Minette, Dipl. Ing. (FH) Daniel Koster, Dipl. Ing. (FH) Oliver O'Nagy

1. Context and abstract

The PV-Forecast project benefits from the financial support of the "Fondation Enovos" (under the aegis of "Fondation de Luxembourg"). "Fondation Enovos" [19] supports for example energy-themed scientific projects with a particular focus on renewable energy, in order to find medium- and long-term solutions that meet both environmental and economic requirements.

The portion of fluctuating, decentralized and not demand side controlled renewable energy sources, such as wind power and photovoltaic (PV), is constantly increasing and will represent a non-negligible part of the near future energy mix.

To ensure grid stability and reliable energy trading, precise predictions of the energy production from these sources will be crucial to ensure grid stability and reliable energy trading. Accurate PV power predictions are not yet widely implemented, but are gaining more importance. The prediction accuracy for larger regions is already very promising, but the drawback is the accurate forecast for smaller regions (i.e. Luxembourg).

The approach described in this article isn't fully developed yet, but the results presented seem to be promising to that end, that the site specific forecasts for the currently available reference systems show good trends, compared to measurement values.

The absolute errors normalized to the nominal power of the systems, for clear weather conditions, do lie under 10%. At cloudy conditions, the forecast performance is substantially lower, due to inaccuracies in the irradiance predictions, as shown later in this article.

The main goal behind this research project is the investigation of possibilities for precise PV power predictions for a small region (or a small country) by a combined approach of predictive modelling of the PV power and the monitoring of reference systems.

Beside the scientific findings, the project would deliver a PV power prediction model for the Grand Duchy of Luxembourg (2'586 km²), adapted to the regional situation, which could be implemented as an online, real-time tool in a final development step.
The project would thereby contribute largely to the future integration of PV into the local power grid and energy mix.

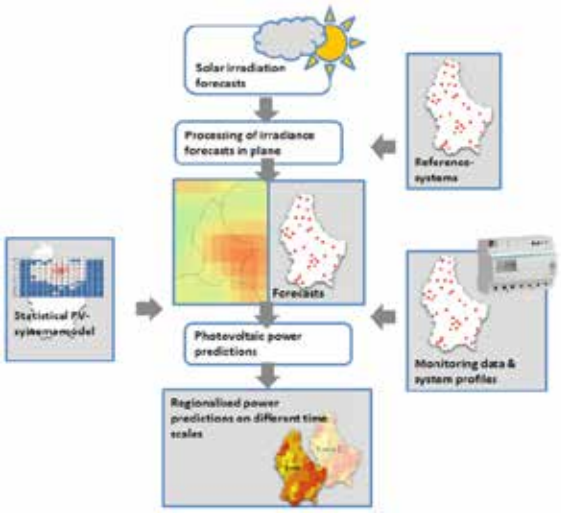

1_ Scheme of the forecasting approach, combining modeling data and statistical information (left hand side) with a feed-back loop from PV reference systems (right hand side)

2. State of the art

Over the last 10 years, the solar irradiance modelling progressed fundamentally and developed application oriented approaches e.g. for energy applications [5]. Beginning from purely meteorological models for solar irradiance prediction, the model developers added physical models that represent PV systems and simulate their performance under the modelled irradiance and temperature conditions. In order to evaluate and calibrate the models, measurement data from real PV systems are being used [3], [4].

Recent studies proved the feasibility of regional PV production forecasts based on intra-day and day-ahead irradiance forecasts given by the ECMWF [3], [7]. The forecast accuracy for single PV installations might vary and is not the purpose of these modelling efforts. The accuracy for larger regions is already very promising (13% for the region of Germany) [4], which proves that these kind of models can generally provide the necessary forecast data. The results show, that local temporal mismatches of predictions and real measured production data, balance out over larger areas. This means, in reverse, that predictions for smaller limited areas show

higher inaccuracies. It is especially this last point (small area, i.e. Luxembourg) which is the focus of our work.

3. Technical approach

The following chapter will explain the technical approach behind the forecasting model shown in Fig. 1.

3.1. Overview of the technical approach

The approach of the PV power forecast within the "PV-Forecast" project is a combination of geo-referenced irradiance and ambient temperature forecast data from numerical weather prediction (NWP) models of the European Centre for Medium-Range Weather Forecast (ECMWF) with measurement data of reference PV systems distributed over the region.

The irradiance forecast data, that can be retrieved from the ECMWF web servers, are processed on our side in order to obtain the irradiance in plane for a matrix of predefined PV system orientations and inclinations and for a number of given PV systems that serve as references. For these reference PV systems, of which measured PV power in a temporal resolution of 15 minutes is available and that are distributed over the whole country of Luxembourg, an individual irradiance forecast in plane of the PV modules is being considered.

Based on individual models for each reference system, representing their technical characteristics, a power forecast for those installations is being generated. The predicted power of the reference systems is compared to their measured generated power with the aim to obtain the base data for a self-adapting model, in the end.

A statistical model of the spatially distributed PV installations in Luxembourg is then used in order to model the generated power for three days on an hourly basis over the whole region. Currently, the spatial resolution of this PV power forecast for whole Luxembourg is the same as the ECMWF irradiance forecast data (0.125° x 0.125°).

3.2. Solar irradiation forecast

For the meteorological part, the PV power forecast is based on a combination of geo-referenced irradiance and ambient temperature forecast data from numerical weather prediction (NWP) models, elaborated by the European Centre for Medium-Range Weather Forecast (ECMWF). Recent studies proved the feasibility of regional PV production forecasts based on intra-day and day-ahead irradiance forecasts given by the ECMWF [3],[7]. The solar radiation data used here is the "surface solar radiation downward" (ssrd, parameter 169 available in grib or netcdf format). This parameter is the incident solar radiation or the so called global horizontal irradiance (GHI) [9].

The solar radiations as well as the temperature forecasts are available at an hourly base up to 72 hours (three days) in advance and with lower time resolution from 72 to 240 hours (10 days). These forecasts are updated twice a day.

The forecast beginning from midnight 00:00 is available 8 hours later (at 08:00) and the forecast for noon 12:00 is available at 20:00. The grid resolution (i.e. longitude and latitude) is 0.125° by 0.125° for one cell. This results for Luxembourg in a North-South resolution of about 14km and in an East-West resolution of 9 km.
Considering that Luxembourg has maximum territorial dimensions in North-South direction of 82 km and in East-West of 57 km (with a total area of 2'586 km2), this results in approximatively 20 cells. One could easily imagine that clouds have a much greater impact here compared to greater regions where the PV power forecasting gives already good results [7]. This smallness of Luxembourg is one of the challenges in the PV-Forecast project.
ECMWF uses a bi-linear interpolation technique. It uses a 2 x 2 grid points closest to the selected interpolation location and takes a weighted average to arrive to the interpolated value [17].

In the definition of the project was foreseen to make a regionalisation of the forecasting data. But it turned out quickly by considering the maximum available resolution of 0.125° that it makes no sense to try to interpolate this already interpolated forecasting data further for getting more areal resolution. Furthermore, in [7], this task was abolished.

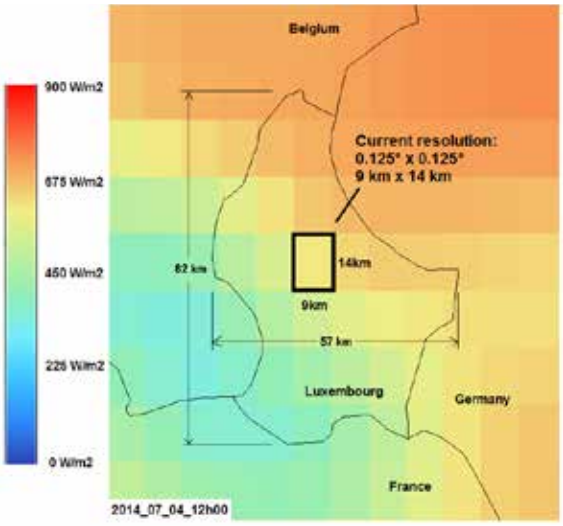

2_ Current available resolution for forecasting data from ECMWF compared to the size of Luxembourg

3.3. Conversion of the global horizontal irradiation forecast value into Inclined Plane Irradation

There are different methods for the calculation of the inclined global irradiation depending on the quantity and quality of available parameters. A rather simple method with a relatively good accuracy published in 1998 by Olmo et al. [6] was finally chosen. A recent study from Khalil et al. [8] points out the simplicity and accuracy of the method developed by Olmo et al. The advantage of this method is that it requires only the global horizontal irradiation GHI, the sun position (elevation to the horizon and incident angle to the inclined surface) and the albedo of the environment.

Calculation of the inclined global irradiation [6]:
$G_\psi = GHI \exp(-k_t*(\Psi^2 - \Psi_H^2))*F_c$

Where:
G_ψ is the inclined global irradiation [Wh/m²];
k_t is the clearness index [-];
Ψ is the incident angle [rad] of the sun to the inclined plane;
Ψ_H is the incident angle [rad] of the sun to the horizontal plane;

GHI is the global horizontal irradiation [Wh/m²];
Fc is the correction factor [-] that is taking the ground reflection (albedo) into account.

The first 3 reference PV systems and the location where the pyranometers are installed are on flat roofs with bitumen, that have a white mineral surface. The albedo factor of 0.35 seems to be appropriate for the calculations during the dry summer months.

A comparison of the calculated values based on GHI measurements with the measured inclined global irradiation (both measurements done with a Kipp & Zonen CM11 pyranometer) shows the relatively good fitting of the trends of both curves, measured and calculated (Fig. 3 and Fig. 4).

However it can be seen that there are deviations of the calculated (blue) values above measured (red) values, that causes an overestimation of the calculated inclined irradiation for clear days. (Fig. 3) The total deviation for this specific clear day is + 9%.

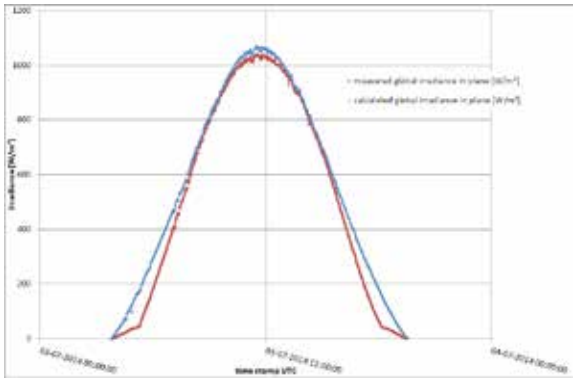

3_ On a clear day in July 2014, measured inclined global irradiance (elevation 30°, azimuth 180° in red) and the calculated inclined global irradiance (blue) using the method developed by Olmo et al. [6].

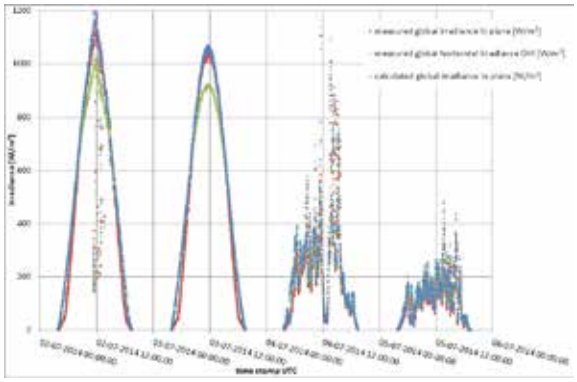

4_ overview on four days in July 2014 with two clear and two cloudy days.

Comparing the pyranometer measurement values at inclined orientation of 30° elevation and 180° azimuth with the calculated values based on GHI measurements, it can be seen, that the variance remains low even under different cloud conditions over a month. Fig. 5 shows the data of July 2014, that was mainly clear (six very cloudy days, five very clear days and twenty predominant clear days). It can be seen, that the calculated values have a low scatter but a systematic deviation in relation to the measured values probably due to the high daily irradiation during the measurement period.

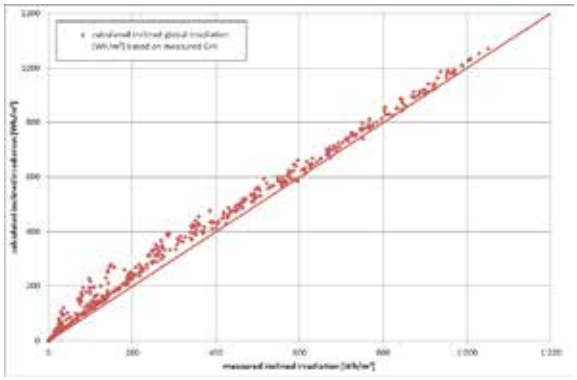

5_ July 2014, calculated inclined global irradiation based on GHI (y-axis) over measured inclined global irradiation (x-axis).

The described calculation method is now applied to the forecast value of the global horizontal irradiation GHI (ECMWF parameter identifier: 169; ssrd). This parameter represents the global horizontal irradiation with the unit [J/m²] (GHI) [9], [10]. There is already a large variance between the ground measured and the forecast data as it can be seen in the Fig. 6. The calculated values are scattered broadly around the measured values.

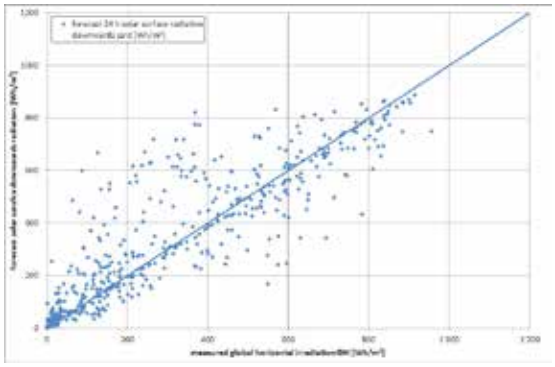

6_ 24 hours forecast ssrd values (y-axis) over ground measured GHI values (x-axis).

The main reasons for this broad scattering can be found in

_forecast accuracy,
_the same forecast area (9 km x 14 km) overlays different microclimate areas, that might have an effect on the ground irradiation,
_inaccurate prediction of cloud distribution and movement in the forecast area (causing variance of the irradiation in both directions: enhancement due to reflection and cloud shading as well as an overlapping of both effects.

The points b) and c) are addressed in this project in order to improve the local forecast

3.4. PV-Power forecasts for the reference systems

It is foreseen to implement a number of reference PV systems into the model. The objective is to obtain a real time feedback from PV systems which are already measured in a high temporal resolution (smart metering) without additional effort, in our case every 15 minutes, in order to be able to adapt the short term forecasting based on this information. At this moment in time, three PV systems are currently characterized and measured, but the aim is to include 30 – 40 systems of a good spatial distribution over Luxembourg.
Each reference system is characterized according to their technical parameters, such as type of PV modules, inverters and cable lengths, inclination and orientation of the PV arrays, age of the installation, location and array setup. After a site visit, the technical model is set up for each system using the following approach:

In the current version, on the level of reference systems, the only pre-photovoltaic losses which are being considered are the reflections on the module surface (no losses due to snow cover or dust). For simplicity reasons, the "ASHRAE incident modifier" was used to account for the reflection losses, although knowing for the limitations of the approach at high incident angles (angle between the normal on the PV plane and the sun rays). To attenuate this effect, the reflection losses at incident angles above 80° have been set to a fixed value of 30%. In a next development step, this approach might change.

The PV modules efficiency has been calculated based on their performance at standard test conditions (STC) and is temperature corrected by the temperature coefficient for the power at maximum power point (MPP). In order to estimate the modules temperature at operating conditions, the following formula was used [3]:

$T_{module} = T_{amb} + \lambda\, G_{\psi}$

T_{module} = module temperature [°C],
T_{amb} = ambient temperature [°C],
λ = 0.020 for free standing PV systems,
0.056 for building integrated PV systems,
G_{ψ} = inclined global irradiance [W/m²].

When calculating the performance based on nominal power, we need to consider the degradation of the modules. During the first year of operation, degradation losses of 2,5% were accounted for [11], [12], [13] and further 0.5%

per year for each additional year of operation [11], [12], [14], [15], which is in good correlation with values found in the mentioned references. Also the mismatch losses of the PV arrays were taken into account by a simple lump sum reduction of 2.5% [18].

In a first version, the inverters performance was considered by applying the European inverter efficiency, as the inverters of the currently integrated three PV systems are rather stable over their operation range. In a next version, when integrating additional reference systems, this aspect will be integrated in dependence on the current part load operation point.

3.5. Statistical model

In order to reflect the circumstance that not all the PV installations have the same inclination and orientation, a so called statistical model was elaborated.

This model is based on statistical data of 6'308 subsidised PV installations out of the Luxembourgish area [2], representing approximately 40% of the installed PV capacity. Only known parameters are considered: installed power and type of module, inclination and orientation angles. It is formed by a distribution matrix with percentages of installed PV-power for the elevation (vertical: 0° to 90° in steps of 5° => 19 classes) and the orientation (horizontal: -180° to 180° in steps of 5°, south = 0°, => 73 classes) for each of the three available module types: mono- and polycrystalline silicon technologies (mono-Si, poly-Si) and other technologies (different thin film materials including amorphous silicon (a-Si), cadmium telluride (CdTe), copper indium gallium (di) selenide (CIGS), etc). Each statistical technology matrix is formed by 73 x 19 = 1'387 values.

As the mono-Si and poly-Si technologies represent more than 98% of the installed power in Luxembourg, only these two where used in the forecasting of the power. Fig. 7 shows a compressed example of this distribution matrix considering all PV module types together.

One can observe that most of the PV installation are south oriented with an elevation of about 30°.

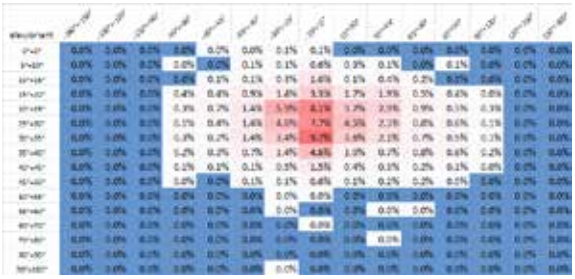

7_ Statistical distribution of the orientation and slope of 6'308 PV systems all over the country

For each forecasted cell in Fig. 2 (defined by longitude, latitude, forecasted solar radiation and ambient temperature) and for each element out of the matrix of Fig. 7 (elevation, orientation, PV technology, percentage of installed PV power, solar incident angle, …) we calculate hourly the generated PV energy and sum them up at the end.

As the statistical matrix is built up with percentages of a certain PV technology, the calculated sum has to be multiplied by the corresponding installed power of this technology in this cell. By this, we obtain a regionalised forecast for each cell of the grid. The sum of all the cells reflects the generated energy for the whole region of Luxembourg for a given hour based on forecasted meteorological data.

If it is desired to transfer the model to another region this input matrix needs to be adapted to the local situation and the regional installed PV capacities.
Fig. 8 shows the installed PV power per commune for PV installations in the Creos grid (2013) with a total installed power of 92'736 kWp.

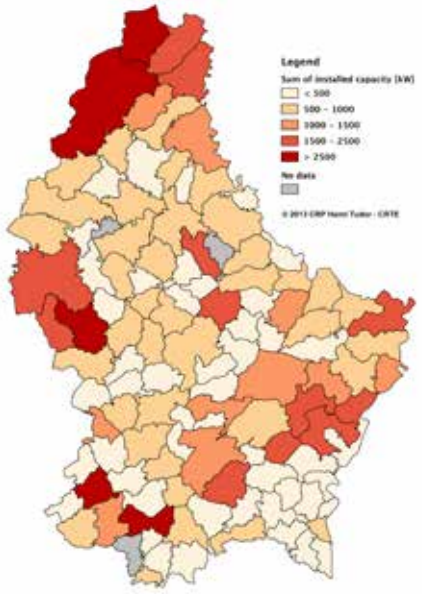

8_ Installed PV-power per commune (Creos grid)

3.6. Adaption of the regionalized forecast by feedback from the reference systems

The final aim of a combined approach of modelling the expected PV power based on irradiance predictions and measurements from reference systems is to increase accuracy and / or spatial resolution. So far, our work hasn't reached the point to give an answer to the question whether, or to which extend this is possible. But we would like to develop and test some of the following approaches and assumptions:

Results from other research groups show, that local temporal mismatches of predictions and real measured production data, balance out over larger areas [7]. This means in reverse, that predictions for smaller limited areas show higher inaccuracies, which is of particular importance to Luxembourg. One of our assumptions is, that on the very short time scale (intra-day) and with appropriate number and distribution of reference systems, it should be possible to identify temporal and spatial mismatches of the forecasts in one part of the region and correct them partially for the coming time steps (3-4 hours).

Comparable to the identification of "cloud motion vectors", a simplified approach could be imagined in order to detect the movement of inaccuracies over the region that are due to temporal mismatches in the predictions. Errors between predictions and the most recent historical forecast can be derived to error maps, in 15 minutes time resolutions. Differences between error maps for the time n and n-1 can indicate direction and speed of such an "error movement".

A study about the operation performance of a large PV system has already used a similar approach to model variations in the incident irradiation due to cloud movement [16].

4. Results

4.1. Comparison of historical irradiation forecast values with measurements of four different locations

The first location that is compared is our outdoor testfield in Esch/Alzette ("PV-Lab") with the ground measurements using high accuracy pyranometers and sun-tracked pyrheliometer. The other three locations are medium sized free-standing PV-systems installed on flat roofs as described in chapter 4.2. The three systems are monitored with reference solar cells (two per system) with an estimated overall accuracy of about +- 10%

PV-Lab outdoor test field:

The total error between forecast and measured inclined global irradiation can be very high because of the large variation between forecast and ground measured data in combination with the low variation that results from

the conversion of the GHI into inclined global irradiation. However the total error will not have a big effect on the PV electricity production, if the irradiation is low. The forecast delivers hourly values within forecast periods from 12 hours to 72 hours. A 24 hour forecast period is applied and compared with the measured values in order to receive a "useful" forecast error. Additionally, the deviations between the hourly calculated forecast and measured value are normalized to 1'000 Wh/m².

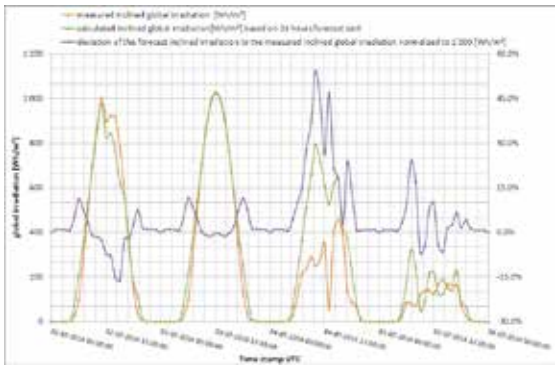

9_ Four days in July 2014: measured inclined global irradiation (orange) and calculated inclined global irradiation (green) based on forecast ssrd. The violet curve shows the deviation between calculated forecast values and measured values normalized to 1'000 Wh/m².

The average of the hourly normalized deviation for the complete month of July 2014 is 9%. The total measured irradiation for July 2014 is 155 kWh/m² while the total forecast value is 186 kWh/m² which results in a difference of 32 kWh/m² or 17% between forecast and measurement.

4.2. Results of the power forecasts for three reference systems

Up to now, the first three reference systems have been chosen, characterized and their system parameter as well as the power metering data has been integrated into the modelling approach. Currently, the contact to further approximately 100 systems is established out of which 30 to 40 systems will be chosen to serve as references.

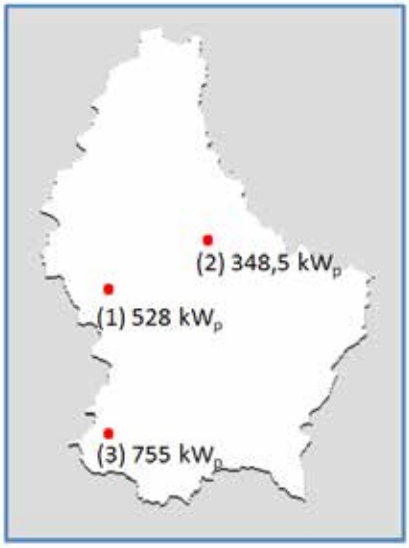

10_ position of the first three reference PV systems

The first three reference PV installations are free standing, crystalline silicon, large scale systems of the following characteristic:

_nominal power: 528.00kWp;
slope: 15° (install. rack) +- 2° (roof inclination); orientation: 219°
_nominal power: 348.48kWp;
slope: 15° (install. rack) +- 5° (roof inclination); orientation: 158°
_nominal power: 755.04kWp;
slope: 20° (install. rack) +- 5°(roof inclination); orientation: 158.5°

4.2.1. Validating PV-Model performance

Beyond the measured electricity, feed-in at the injection point, we got access to the data acquisition server of the three installations and retrieved the measured irradiance data on site. Those values were measured by reference cells installed in plane with the PV modules.
In order to validate the quality of our PV system model, independent from the quality of the irradiance forecasts, we used the measured "irradiance in plane" from the reference cells as input for our model and compared the results for one month (July 2014) with the measured energy yield data from smart meters (see Fig. 11 as an example).
The four days show a comparably well correlation of the modelled PV yield with the measured data. We observe slight overestimations of the model at clear weather conditions and slight underestimations at cloudy conditions.

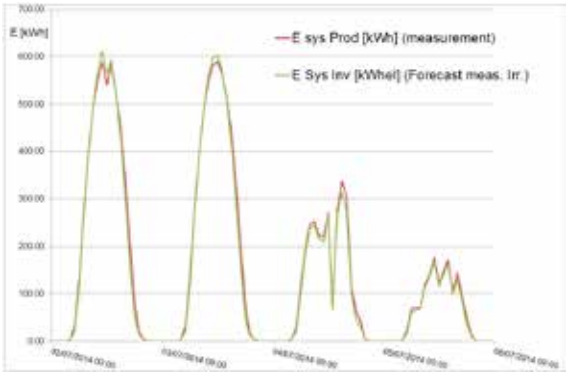

11_ comparison of measured energy yield data (red) of PV system (3) to modelled energy yield (green), using the irradiance measurements of reference cells as model input, for four days in July 2014

For reasons of data availability for the reference systems, the modelling results could until now only be evaluated for the time span of one month (July 2014). For this month, the deviation of the modelled yield (monthly sum) to the measured yield was -3.9 % of the measured value for system (1), -2.4 % for system (2) and -3.2 % for system (3), meaning an underestimation of the systems real performance.
The mean deviations of the modelled daily sums to the measured daily sums are -4.2 % for system (1), -2.4 % and -3.6 % for system (2) and (3).

Looking at hourly data, the picture becomes much more divers. The accuracy of the modelled hourly PV power, as compared to the measurement is being assessed by the relative error compared to the measurement and by the absolute error, normalized to the nominal power of the PV systems (both approaches are explained further down in 4.2.2).

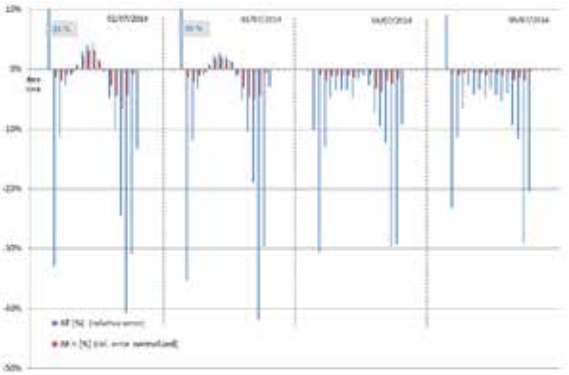

12_ comparison of the relative error of modelled hourly PV power (blue) of PV system (3) and the absolute error normalized to the nominal power of the PV system (red) (using the irradiance data from the reference cells as model input, for four days in July 2014)

Fig. 12 shows, that the PV model generally underestimates the system performance, with higher deviations at high inclination angles. Especially the high inaccuracies in early and late hours over the day, at relatively low irradiations, result in a high relative error but being less important considering the low absolute energy values for those hours. This is illustrated by the red curve - the absolute error, normalized to the nominal power.

4.2.2. Validating the full forecast models performance

After having assessed the forecast accuracy of the irradiance forecasts including the processing of in plane data (4.1.) and the quality of the PV system model (4.2.1), we assessed the full model, from irradiance forecasts to the PV power forecast for the reference systems by comparing it to the measured yields as well:

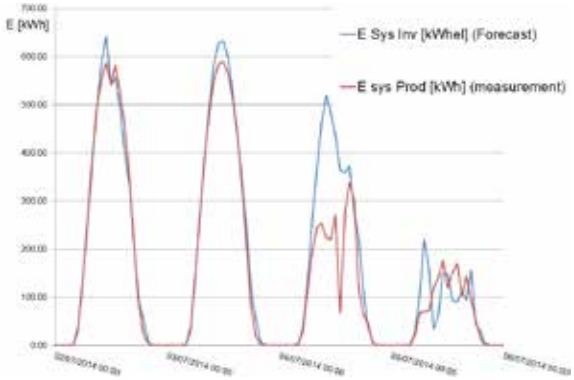

13_ comparison of measured energy yield data (red) of PV system (3) to modelled energy yield (blue), using the irradiance forecasts from ECMWF, for four days in July 2014

Fig. 13 illustrates a general tendency, which is clear from what we know about the irradiance forecasts already. The model seams to predict rather well the PV power at clear weather conditions (02/07/14 and 03/07/14), while at cloudy conditions (04/07/14 and 05/07/14) the predictions can deviate substantially from measurements.
Expressed in numbers, the picture is the following:
Also for July 2014, the deviation of the forecasted yield (monthly sum) based on solar irradiation forecasts to the measured yield was 10.2 % of the measured value for system (1), 13.7 % for system (2) and 11.0 % for system (3), meaning an overestimation of the real yield.
The mean deviations of the forecasted daily sums compared to the measured daily sums are 13.6 % for system (1), 17.6 % and 14.7 % for system (2) and (3). Those values are given just for reasons of completeness but should be taken cautiously, as the variance for daily sums is rather high. They mainly give an idea about the bias, which is (for July) an overestimation of the real system yield.
The final objective is obtaining reliable hourly forecast values, which is a much more difficult endeavour. Fig. 14 shows the relative error for the same four representative days as used before. The relative error has been calculated in relation to the real power of the system:

$\Delta E\,[\%] = (E_{sys\,Inv} - E_{sys\,Prod}) / E_{sys\,Prod}$

$\Delta E\,[\%]$ = relative error of hourly PV power forecasts,

$E_{sys\,Inv}$ = hourly power forecast of the PV system behind inverter,

$E_{sys\,Prod}$ = hourly measured power of the PV system.

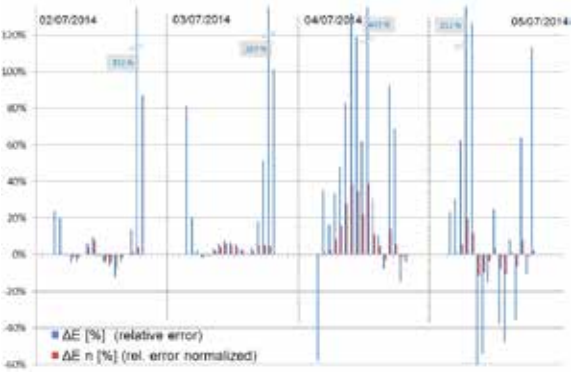

14_ comparison of the relative error of forecasted hourly PV power (blue) of PV system (3) and the absolute error normalized to the nominal power of the PV system (red) (using the irradiance forecasts from ECMWF, for four days in July 2014)

The Fig. 12 shows a rather good forecasting performance (relative error in blue) for days of clear weather conditions (2nd and 3rd of July), which is not surprising keeping in mind what we assessed before. On cloudy days, the results are more divers and worse in the overall general performance, what can be shown by the values for the 4th and 5th of July.

Especially for the values at clear weather conditions, it became obvious that the relative error increases at high incident angles (in the morning and at evening) when the overall power is already rather low. Here, obviously, a relatively small absolute error leads to high relative deviations. Therefore, we assess the forecast values also by normalizing the absolute error of the forecasts to the nominal power of the respective PV system:

$\Delta E_n\,[\%] = (E_{sys\,Inv} - E_{sys\,Prod}) / P_n$

$\Delta E_n\,[\%]$ = normalized absolute error of hourly PV power forecasts

P_n = nominal power of the PV system

Fig. 14 also shows this normalized absolute error (in red) and illustrates well that the performance of the forecast for days of good weather conditions is already quite promising (error generally below 10%). At cloudy conditions, the normalized absolute error can reach values of 50% at maximum in our sample of one month, but normally stays well below 35%.

5. Conclusion

Within this project, unlike most other existing models, the reference systems do not only serve as a basis to upscale PV-production data for the forecast-area. The reference systems are being continuously monitored and deliver data for refinement of the forecasts.
The described approach contains a set of existing and proven models ranging from the processing of the irradiance forecasts, to the behaviour of the PV reference systems.

Using the model described by Olmo [6] to calculate the inclined surface irradiation out of the horizontal irradiation forecasts, performed well, but showed a slight positive bias, that we will further investigate as this behaviour doesn't correspond with the experiences of other research groups reported in the literature [8].

We assessed the performance of the PV model that calculates the hourly PV power of the reference systems and found that the model represents the actual performance rather well, although we had slight deviations which can be further reduced by calibration of the model.

When comparing the actual performance of the full forecasting model (using intra-day irradiance forecasts) for the three currently included reference systems, we find good correlation in time, at clear weather conditions.

At cloudy conditions, PV power forecasts for the single site can deviate substantially from the real measured power, due to inaccuracies of the irradiance forecasts, mainly.

In order to correct our forecasts in the short term forecast horizons by the experience from the comparisons for the reference systems, we need a broader basis of reference systems, which we have not yet available. In the near future, the described adaptation approach can be further elaborated and evaluated for its performance.

6. Outlook

The next step in the development of the described forecasting model is the choice, characterisation and inclusion of further PV reference systems (up to 40), that will allow for the calculation of the mentioned error maps.

This will enable the evaluation of the technical part of the model for a higher number of systems. Also, the evaluation of the approach needs to be done in reference to monitoring data over a broader time period and for different forecasts horizons, 2- to 3-days ahead.
All the different reference systems will be analysed in order to identify systematic over- or underestimations by the technical part of the model, which we could minimize by calibration.

Once sufficient reference systems are included and error maps for a larger time period are available, the technique to identify error patterns, their direction and speed of propagation over the forecast area, will be further developed.

7. Acknowledgements

Fondation Enovos for the financial support. CREOS, ENOVOS and their customers for providing measurement data of the reference PV systems, the Luxembourg Environment agency for providing statistical data, the ECMWF for giving access to the forecast data and our colleagues Christian Braun, Jonathan Hervieu and Markus Jonas (CRP Gabriel Lippmann) for the processing of the forecast data.

REFERENCES

1_ F. Minette, D. Koster, O. O'Nagy, 2014, PV-Forecast: Regionalised Forecasting of Energy Production from Photovoltaic and Their Dynamics by a Combined Approach of Modelling and Real Time Measurements of Reference Systems, Pages 2225 – 2232, ISBN: 3-936338-34-5, Paper DOI: 10.4229/EUPVSEC20142014-5AO.8.5

2_ Anonymised Data from the Luxemburgish "Ministère du Développement durable et des Infrastructures > Administration de l'Environnement > Division de l'Air et du Bruit > Service Registre des économies d'énergies"

3_ E. Lorenz, T. Scheidsteger, J. Hurka, D. Heinemann, C. Kurz; 2010, Regional PV power prediction for improved grid integration; ISBN: 3-936338-26-4, 25th EUPVSEC 2010 - 5AO.8.1

4_ Lorenz, E.; Hurka, J.; Heinemann, D.; Beyer, H.G., 2009, Irradiance Forecasting for the Power Prediction of Grid-Connected Photovoltaic Systems; Selected Topics in Applied Earth Observations and Remote Sensing; IEEE Journal, vol.2, no.1; pp. 2-10

5_ Dunlop, E. D.; Wald, L.; Súri, M., 2006, Solar energy resource management for electricity generation from local level to global scale; Nova Science Publishers; ISBN 1594549192

6_ F.J. Olmo, J. Vida, I. Foyo, Y. Castro-Diez, L. Alados-Arboledas, 1998, Prediction of global irradiance on inclined surfaces from horizontal global irradiance, Energy 24 (1999) 689–704

7_ Photovoltaic and Solar Forecasting: State of the Art, IEA PVPS Task 14, Subtask 3.1, Report IEA-PVPS T14-01: 2013, October 2013

8_ Samy A. Khalil, A. M. Shaffie, 2013, Performance of statistical comparison models of solar energy on horizontal and inclined surface , International Journal of Energy and Power (IJEP) Volume 2 Issue 1

9_ Alberto Troccoli, Jean-Jaqcues Morcrette, autumn 2013, ECMWF Newsletter 137

10_ Patrick Mathiesen and Jan Kleissl, 2011, Evaluation of numerical weather prediction for intraday solar forecasting in the continental United States, technical report of the Department of Mechanical and Aerospace Engineering, University of California, San Diego

11_ Quintana, M.A. ; King, D.L. ; McMahon, T.J. ; Osterwald, C.R., Photovoltaic Specialists Conference, 2002. Conference Record of the Twenty-Ninth IEEE, Commonly observed degradation in field-aged photovoltaic modules

12_ Sakamoto, S., Oshiro, T., 3rd World Conference on Photovoltaic Energy Conversion, 2003, May 2003, Vol.2, pp.1888-1891, Field test results on the stability of crystalline silicon photovoltaic modules manufactured in the 1990s

13_ Dunlop, E.D., 3rd World Conference on Photovoltaic Energy Conversion, 2003, May 2003, Vol.3, pp.2927-2930, Lifetime performance of crystalline silicon PV modules

14_ Skoczek, A., Sample, T. , Dunlop, E.D., Progress In Photovoltaics, 2009(4), pp.227-240, The Results of Performance Measurements of Field-aged Crystalline Silicon Photovoltaic Modules

15_ De Lia, F.; Castello, S.; Abenante, L., Proceedings of the 3rd World Conference on Photovoltaic Energy Conversion, 2003, Vol.B, pp.2105-2108, Efficiency degradation of C-silicon photovoltaic modules after 22-year continuous field exposure

16_ P. Öchsner; M. Zehner; F. Lang; T. Rauscher; J. Weizenbeck; T. Weigl; G. Becker; G. Bettenwort; B. Giesler; T. Betts; R. Gottschalg, 28th European Photovoltaic Solar Energy Conference and Exhibition 2013, spatial modelling of grid connected PV plants with 3D irradiance values

17_ Persson Anders, October 2011, User guide to ECMWF forecast products, 127 pages

18_ J. Webber and E. Riley, Mismatch Loss Reduction in Photovoltaic Arrays as a Result of Sorting Photovoltaic Modules by Max-Power Para meters, ISRN Renewable Energy Volume 2013, Article ID 327835, 9 pages

19_ Fondation Enovos: http://www.fondation-enovos.eu/en/index.php

This article is based on our results presented on the 29th European Photovoltaic Solar Energy Conference and Exhibition (EU PVSEC 2014) held in September 2014 in Amsterdam and published in the EU PVSEC 2014 Proceedings [1]

Within the EU project CockpitCI "Cybersecurity on SCADA: risk prediction, analysis and reaction tools for Critical Infrastructure" and under the patronage of Étienne Schneider, Minister of Economy and Foreign Trade, itrust consulting and CREOS, organised the 3rd CockpitCI Workshop on "SCADA Cybersecurity" at Creos' national dispatching centre on March 10th,, 2014.
This workshop enabled the European Union Agency for Network and Information Security ENISA, Luxembourgish authorities (Ministry of Economy, GOVCERT.LU, HCPN), the national electricity and gas operator CREOS and other Luxembourgish industrial attendees as well as the project partners to discuss problems and solutions on the security of critical infrastructures.

New security technology to face cyberattacks

COCKPITCI: HOW TO MONITOR CYBERRISKS ON A CRITICAL INFRASTRUCTURE?_

Dr. Carlo Harpes, Matthieu Aubigny Ing.

CockpitCI gave itrust consulting the opportunity to develop two software products: a meta anti-virus appliance called AVCaesar and a software version monitoring tool called Software Checker.

This article explains the context of Critical Infrastructure protection, the political ambition and practical risk to achieve this. Some results of CockpitCI are given, and a follow-up project, called Smart Grid Luxembourg Cockpit aiming to tailor security for the future network of smart electricity meter in Luxembourg is announced.

1. Critical Infrastructure Protection

1.1. CI as target for attacks

Critical Infrastructures (CI) like electricity, gas or water distribution systems, and train or airplane controlling system are vital for the functioning of national and European organisations and industrial sectors. They should stay, at least partially operational, even in the event of serious dysfunctions due to natural disasters or malicious attacks. Nowadays, such infrastructures have become a target of cyber-attacks. The research experiment Aurora and recent attacks (Stuxnet, Duqu, Red October) have shown that all these networks and underlying industrial systems are potentially vulnerable to attacks. The Stuxnet malware ruined almost one-fifth of Iran's nuclear centrifuges, which are based on IT systems generally considered as well-protected, well segregated, and immune to cyber-attacks.

1.2. "Blackout"

The famous novel "Blackout" by Marc Elsberg describes the consequences of a cyber-attack shutting down the entire electrical supply of Europe. This fictional novel is based upon solid investigations on the functioning of the European electrical grid and its present vulnerabilities. The book describes the impossibility of detecting the causes and sources of the problem quickly enough, and it illustrates that the measures to prepare the population for the coming disaster have been insufficient.

1.3. The political aspects

Since 1990s, specific services have been considered as essential to maintain industrial activity in a country and even to ensure the way of live for its citizen. In that aim, most of industrial countries as USA and European countries have decided to establish the list of such services and to apply security measures to ensure their reliability. These services, which encompass energy distribution (electricity, gas, oil), emergency services, financial services, telecommunication, space services, have been called "critical" in a specific framework, the Critical Infrastructure Protection (CIP).
In the European Parliament resolution of 12 June 2012 on critical information infrastructure protection – achievements and next steps: towards global cyber-security, the European Parliament

_"welcomes the Member States' implementation of the European Programme for CIIP , including the setting-up of the Critical Infrastructure Warning Information Network (CIWIN), […]
_acknowledges that the Commission is considering revising Council Directive 2008/114/EC and calls for evidence to be provided of the effectiveness and impact of the directive before further steps are taken, […]
_considers that ENISA can play a key role at European level in the protection of critical information infrastructure by providing technical expertise to Member States and European Union institutions and bodies".

Even if the text underlines the will of European parliament to support CIP, we interpret this text as a sign that the EU has limited authority to improve CIP. In respect of national sovereignty for security matters, they rather encourage this to be done at national level, as can be seen form recent publications:
1. In the setup of the Critical Infrastructure Warning Information Network (CIWIN), the EU aim is defined as follows: "with the help of assisting Member States to exchange information on vulnerabilities and appropriate measures and strategies to mitigate risks related to CIP". Originally, CIWIN intends to be an alerting system, but not only an information sharing system. This alerting has been postponed to a second phase.
2. In the proposal for a directive concerning measures to ensure a high common level of network and information security (NIS) across the Union: "This will be achieved by requiring the Member States to increase their preparedness and improve their cooperation with each other, and by requiring operators of critical infrastructures, such as energy, transport, and key providers of information society services (e-commerce platforms, social networks, etc), as well as public administrations to adopt appropriate steps to manage security risks and report serious incidents to the national competent authorities." (cf. COM(2013) 48 final of 7.2.2013).
However, as demonstrated by the Stuxnet malware, the complexity of such an attack exceeds any national level.

1.4. The challenges

Indeed, two lessons should be derived from recent attacks: first we need better care on security and risk management of Critical Infrastructure. Secondly, as prevention cannot be perfect, we should better monitor security aspect to detect and block cyber-attacks, or at least, to mitigate their impact on the entire systems.

Marc Elsberg's novel illustrates well the consequences of unwillingness by national regulator and private operators to alert or shared their information on risk with other entities.

To face these challenges, political decisions cannot provide quick solutions. The ball is in the court of security experts and CI operators to find relevant, smart and economic sustainable solutions to improve their security.

2. A specific response: the CockpitCI project

2.1. CockpitCI project genesis

In a previous research project, called MICIE; with a focus on electricity grids, we concluded that it is imperative to design systems which allow operators to assess the operational risks, to promptly communicate such risks with interested parties, so that they can prepare suitable containment and prompt risk treatment.

At the end of this project, itrust consulting together with most research partners of MICIE defined a new project proposal to apply lessons learned to Cybersecurity. This proposal was retained for funding by the EU Commission.

The European research project CockpitCI, acronym for "Cybersecurity on SCADA : risk prediction, analysis and reaction tools for Critical Infrastructures" started in early 2012. With a total cost of 4,3 Mio € of which almost 3 Mio are funded by the EU, the project aims to create a framework and tools enabling the detection, analysis, and real-time information sharing of cyber-attacks in order to assess risks and avoid disastrous cascading effects.

2.2. itrust involvement in the project

Within CockpitCI, itrust consulting participates in the description and modelling of the cyber-attacks, modelling and prediction of Quality of Service, in the development of parts of the analysis tool, in the design of security requirements and operational requirements of the Secure Mediation System, and in trial and dissemination. itrust leads the dissemination by organizing workshops, hosting and feeding the website, organizing demonstrations for CI operators.

As preliminary results, itrust consulting has developed two detection probes of the CockpitCI tool, which can also be used as independent tools: AVCaesar and Software checker.

2.3. A meta-antivirus: AVCaesar

AVCaesar is a meta-antivirus that combines several antivirus programs that perform an in-depth scan of any file exchange between sensitive networks like SCADA and IT, and the corporate networks often linked to the internet. This tool can also be used by security incident analysis teams in order to scan and pre-analyse suspicious files.

AVCaesar can be used to:
_Perform an efficient malware analysis of suspicious files based on the results of a set of antivirus solutions, bundled together to reach the highest possible probability to detect potential malware;
_Search for malware samples in a progressively increasing malware repository managed by malware.lu CERT, a brand of itrust.
_Generate an incident report in a specific format (i.e. IDMEF format) to feed automatic analysis tools as in CockpitCI PIDS (Perimeter Intrusion Detection System).

The tool currently integrates antivirus tools like Avast, AVG, Avira, ClamAV, Emsisoft, ESET NOD32, GData, Kaspersky, McAfee, Microsoft Essential Security.

In future, AVCaesar can also be installed as software appliance in the security infrastructure of CI operators.

2.4. Vulnerability detection agent: software checker solution

After installation of a light software client on machines spread over the monitored network, Software Checker informs a server integrated in the CockpitCI tool, on the installed software, key elements of the configuration, and potential vulnerability of the software according to vulnerability databases like OSVDB. This is an essential input for assessing the risk level, but also a starting point for detecting installed malware.
The first version of Software checker verified whether Windows operating systems contains software with security vulnerabilities and warns whether updates of software are available. Future versions will allow managing this information centrally, collecting information from Unix system and even embedded system, and using it for predicting potential attack, and also for planning upgrading actions.

3. 3rd CockpitCI Workshop on "SCADA Cybersecurity" in Luxembourg.

On March 10th 2014, itrust consulting and CREOS, under the patronage of Étienne Schneider, Minister of Economy and Foreign Trade, organised the 3rd CockpitCI Workshop on "SCADA Cybersecurity" at Creos' national dispatching centre.
This workshop enabled the European Agency for cyber security, Luxembourgish authorities (Ministry of Economy, GOVCERT.LU, HCPN), the national electricity and gas provider CREOS and other Luxembourgish industrial attendees as well as the project partners including the security consultancy and research company itrust consulting, the CRP Henri Tudor from Luxembourg, the project coordinator Selex ES from Italy, Romanian operators, and researchers from Italy, Portugal, Great Britain, Israel, Norway and Belgium to discuss the problems and solutions concerning the security of critical infrastructures.
As opening talk to the workshop, the authors of this article referred to new security standards in this domain like the IEC 62442 family and to the importance of communicating risks between CI professionals and being prepared in order to react effectively in case of an attack.
Mr François Thill of the Ministry of Economy assured the audience of the Ministry's support to all Luxembourgish initiatives focusing on acquiring the necessary competencies in order to protect the electricity, gas and water supply against malicious attacks.
Carlo Bartocci, responsible of Creos' dispatching, spoke about technical problems encountered during the migration of their current control management system. The improved performance of supervision systems makes them increasingly more complex and thus it is more difficult to find flaws, being it unintentional errors like simple technical incompatibilities or even worse intentional threats like a malware. His presentation highlighted why it is extremely important to protect SCADA networks from the open telecom network, why data flows should be traced, why functional and security tests before changing are mandatory, and when detailed monitoring is needed.
Adrian PAUNA, NIS expert at ENISA, presented several European initiatives: first, ERNCIP aimed at sharing knowledge to harmonise test protocols, second, the recommendations to use security certified products, and third, the recent project for cybersecurity skills certification of SCADA experts. He invited all experts to participate in their ICS SCADA Expert Group.
Paul Rhein, Haut-Commissariat à la Protection National (HCPN), presented Luxembourg's governmental actors in cybersecurity, like the CERTs, and their coordination bodies. A new law should increase the importance of cybersecurity and crisis preparedness, as a reaction to the fear expressed by the EU commissioner Neelie Kroes that "self-regulation does not work here".
In the second part of the workshop, Antonio Graziano from Selex ES, Italy, presented the CockpitCI project. He compared the new cyber threats on control systems with an F16 jet attacking a WW1 battlefield. The CockpitCI system under

construction should be a decision making system in passive mode; detecting, analysing and managing cybersecurity risk in real time. Prof Paulo Simões, University of Coimbra (Portugal), explained a main part of the system, i.e. the detection architecture: In a distributed network, probes bring security information from IT networks, Operator networks, and Field networks to the Security Management Platform. These probes or detection agents are part of smart perimeter intrusion detection systems (PIDS), including HIDS, NIDS, fieldbus honeypots, software and configuration checkers, etc., and analysis tools such as correlators or OSVM engine (cf. figure). Prof. Stefano Panzieri, University of Roma Tre, illustrated the On-Line Risk Prediction System. He discussed interdependency models, knowledge bases with countermeasures, risk assessments, etc., to process the detected information. If needed, this system alerts and proposes counter-measures to the control centre through a so-called Cockpit. Prof. Michele Minichino from ENEA Italy illustrated the underlying models established in CockpitCI for an electrical grid, for the virus spreading over this grid, and for the Fault, Location, Isolation and Restoration system (FSIR) behaviour in case of virus attacks. Prof Leandros Malgaras from the University of Surrey (UK) presented a tool for the consolidation of detection information based on "One Class Support Vector Machines" (OCSVM).

Finally, itrust consulting demonstrated for the first time two tools it has developed under CockpitCI: AVCaesar and Software Checker.
In the after-workshop-discussion, the participants discussed the importance of developing complementary competencies which enable the detailed analysis of sophisticated cyber-attacks. itrust consulting, which is operating the first private CSIRT (Computer Incidence Response Team) in Luxembourg, called "malware.lu CERT", and which is in partnership with CIRCL and GOVCERT.LU is motivated to assist control system operators in this challenge.

4. Smart Grid Luxembourg – Cockpit (SGLC)
As a follow-up of CockpitCI, some national actors: itrust consulting, Luxmetering GIE, and CREOS, as well as the interdisciplinary Centre Security, reliability and Trust (SnT) of the University of Luxembourg, decided to launch a project to develop a real-time cyber risk monitoring tool, primarily dedicated to monitor the security of the future national smart grid. The project is co-funded by the Ministry of Economy and aims to finish in 2016 with a security monitoring tool acting passively on the smart-metering management system. As such it intends to provide an overview on security and operational risk, to be used by security management, independently of the manufacturer, the integrator, and the team of operators of the smart-metering managing system.

SGLS aims at modelling, developing and testing tools and techniques for monitoring cyber-security aspects of smart-meters in the context of the Luxembourg Smart Grid Project (SGL 2.0). These tools and techniques could then be used to manage and control the security of the smart meters that will be installed in the Luxembourgish grid. The use of these tools is not limited to smart grid. Indeed, they could be extended to address the need of other operators of critical infrastructure (e.g. water grid operator) which could also be the target of cyber attacks.

Moreover, the research collaboration aims at combining security risk analysis with real time indicators based on measures on the operational infrastructure. For this reason, the Cockpit SGL project consists in completing the existing basic security architecture by relying on a risk analysis approach, which will use real time indicators of the level of cyber security risks. In addition to this, a new security events detection system will be put in place, based on the deployment of an intrusion detection system that will monitor during real-time and raise alerts when potential attacks are detected. These two main components (the risk analysis element and the event detection element) will be located in the same central supervision and management system.
In particular, the project will focus on the hacking of smart meters under test in Luxembourg. This type of hacking could be the first vector attack to a deeper attack targeting vital systems located in smart grid system. In that aim, the project will perform:

_Analysis of malware targeting first smart meter and secondly systems and devices belonging to critical infrastructure network
_Modelling, research and implementing of detection mechanisms
_Adaptation of malware.lu CERT to the specificities of smart meters.
The logical functions of the supervision tool are illustrated in following figure:

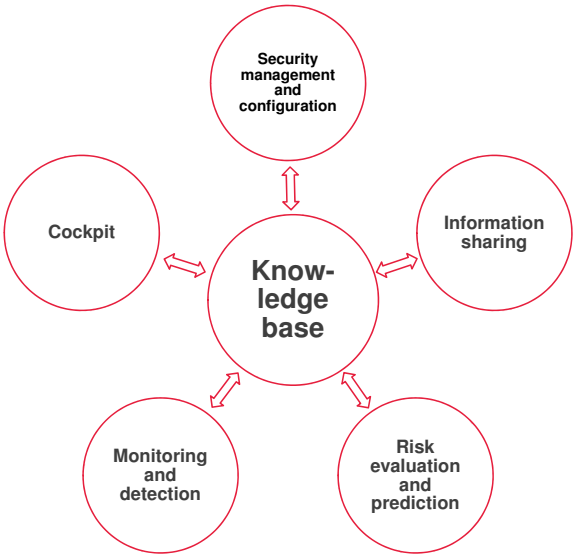

5. Outlook
Protection of critical infrastructure has been recognised as a priority, at EU and national level. In a series of research projects including participation from Luxembourg, methods and technology for better protection are being developed. Several actors, thanks to EU and national funding, deal with developments of appropriate and better security than what is operated today.

Whether these security measures will be deployed depends on the society readiness to pay for security. Today's population has never lived a longer period without electricity, without gas, without telecommunication, without internet or banking services, or most important without food or automatic water provisioning. It has never lived other situations than peace and public control. This, however, is not a default situation; it needs protection; it has a price to pay for. Natural disasters, like the tsunami in Fukushima, have created in the past greater damages than deliberates attacks. Nevertheless, cybersecurity, research results, or recent tests, like stress test on nuclear power plant, demonstrate the feasibility of high damaging attacks, and the still insufficient protection against cyber attack. Predicting such risk is difficult. For natural disaster we can use statistical evidence to estimate the probability of occurrence. For cyber-attacks, this is far more difficult, as there cannot be historic evidence.

Mutual trust and readiness to share knowledge is a prerequisite of effectively managing the next cyber-attacks. Insiders know that security has a price, not negligible, but far lower than the impact of attacks. They also know that past resources have been insufficient to counter serious attacks. Pessimists claim that 100% security is not possible, and they often try to abuse this argument to justify an ineffective security or stagnation of today's countermeasures. But if 100% security is not possible, to decrease the impact of such risks by effective counter-measures is handy.
Critical Infrastructure Protection is mandated by social responsibility. Protection against cyber-attacks merits more public attention, to make sure that interested parties, in particular all citizen benefitting from our economically wealthy situation, are ready to invest resource in protecting them against all kind of malicious intentions.

www.itrust.lu

1_CIIP = Critical Information Infrastructure Protection, is the ICT related part of CIP, dealing in particular with cybersecurity, e.g. attack from Internet.

2_ENISA = European Union Agency for Network and Information Security, originally European Network and Information Security Agency, created in 2004 by EU Regulation No 460/2004.

The demand for hybrid polymer-metal structures is continuously growing due to their great potential in automotive, aerospace and packaging applications. The expected capabilities are highly diverse and include functional, chemical and mechanical as well as economical and ecological aspects. A novel laser beam joining process for hybrid polyamide-aluminum structures is reported. The spatial and temporal heat input is optimized for optimal bonding quality. At the interface it was proven that the polyamide was not decomposed as a result of excessive thermal stress. It was shown that laser or electro-chemical surface pre-treatment of the aluminum substrate has a distinctive effect on the shear strength of the joint. However, the bond quality does not correspond to a change of surface roughness. Therefore, mechanical interlocking in direct relation to surface topology of the pre-treated substrate is not the principal cause for the bonding phenomenon. Chemical analysis in terms of IR-spectroscopy has shown a physicochemical interaction based on hydrogen bonds.

8th International Conference on Photonic Technologies LANE 2014

LASER ASSISTED JOINING OF HYBRID POLYAMIDE-ALUMINUM STRUCTURES_

M.Eng Christian Lamberti, Prof. Dr.-Ing Peter Plapper, Dr. Tobias Solchenbach, Prof. Dr. rer. nat. habil. Wulff Possart

Polymers, often believed to compete with steel and aluminum, have been established as being complementary to metals among the most important engineering materials, Klein (2013). Especially in automotive and aerospace industries both light metals and plastics are being extensively used for lightweight products. The choice largely depends on the requirements that have to be met, with each material offering specific qualities that do not correspond with the other.
During the last years a great potential has been recognized in the development of hybrid structures, Kelly (2004); Michaeli and Hoffmann (2009). The strategy follows the wish to combine specific material-related properties within highly integrated and lightweight structural components to take advantage of the specific functional, chemical, electrical and mechanical as well as economical and ecological aspects of each material. Weight reduction and corrosion prevention of exposed construction parts are of particular importance, while stability, bonding strength and design must be guaranteed or even further improved.

However, the bonding of dissimilar materials remains the technical challenge. Various processes have been developed, including mechanical, adhesive and thermal joining, Mitschang and Velthuis (2008); Wirth (2011); Balle et al. (2008). The use of heavy mechanical connecting elements like bolts or rivets are not in line with the general understanding of light-weight design. In addition, scattered single attachment points do not contribute a uniform load distribution between the adjoining materials by generating local stress peaks. Adhesive glues often contain environmentally harmful or health-endangering solvents and require curing time before handling of the joined components.

First approaches have been developed during research activities focusing on laser joining of metals and plastics which can be further distinguished into two categories: mechanical interlocking and physicochemical bonding. The first approach makes use of patterns of grooves with undercuts in sub-mm-scale at the metallic surface, generated by a focused laser beam, Amend et al. (2013); Roesner et al. (2011); Flock (2011) are being used. Subsequently to the structuring of the substrate, the thermoplastic polymer is being molten onto the metallic substrate, heated by a second laser irradiation. After resolidification both materials create a mechanical link. The second effort uses a line focused laser beam to join the overlapping sheets, Jung et al. (2013); Wahba et al. (2011); Farazila et al. (2011); Fortunato et al. (2010); Katayama and Kawahito (2008). The irradiation heats the metallic surface either directly or through the transparent plastic material which in turn melts the polymer via heat conduction. In both cases the metal remains solid. A SEM/TEM analysis has proven a tight bond between both materials. Furthermore, the appearance of gas bubbles inside the molten polymer has been reported which indicates a thermal degradation. Common for all investigations, the substantial amount of the laser energy is absorbed by the metallic partner.

Strategy

The present paper demonstrates the laser joining of polyamide 6,6 and aluminum without the use of adhesives or previous mechanical surface processing. These materials were chosen based on industry feedback, to address representative industrial requirements. Although polymers and metals generally have a dissimilar chemical structure, physicochemical bonding is expected to take place on molecular or atomic level, respectively, based on the enhanced reactivity of the metal boundary layer with the molecular species present in the polymer, Nikolova (2005).

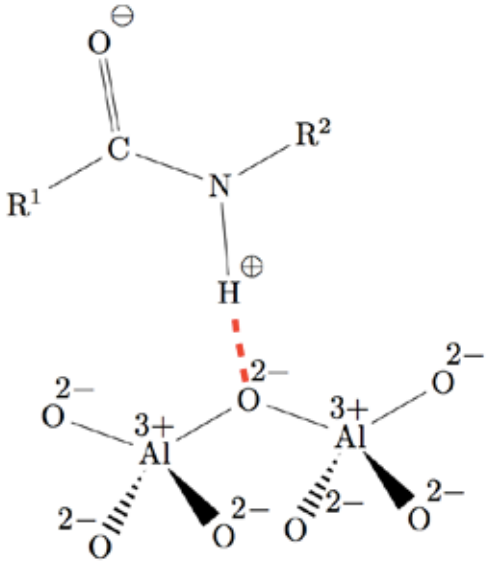

1_Hydrogen bond

Fig.1 shows a hypothetical bond between a polyamide molecule and the ionic aluminum-oxide structure. The local displacement of electrons caused by covalent bonds between non-metallic elements of different electron affinity (C, O, N and H) creates unevenly charged segments within the polyamide molecule which is characteristic for this polymer, Brockmann (1987); Briehl (2008); Dominighaus et al. (2012). The resulting dipole momentum enables the polymer chains to interact with their immediate environment by forming secondary bonds at these distinct anchor points. However the strength of these bonds strongly depends on their length and angle. In molten state, the polymer chains are able to change their conformation and orientation towards the metal surface to support the formation of hydrogen bonds as one possible form of interaction.
For verification of the bonding quality specimen were prepared for tensile shear tests and the maximum load was evaluated. Furthermore, infrared spectroscopy (FTIR) analysis was performed to prove physicochemical interactions at the fusion zone between both materials.

Laser Beam Joining Process

The significantly lower melting temperature of the polyamide starting around Tmelt = 255°C and particularly its decomposition starting already below temperatures of 400°C compared to aluminum melting at T_{melt} = 660°C excludes the application of a conventional welding process. Preparatory experiments have shown that a starting liberation of gas in the polymer melt must already be expected at a temperature of approximately 330°C. The upper limit of the temperature at the interface must be lower than the decomposition temperature of the polyamide. All this demonstrates the importance of a well defined heat input. To achieve the required precision, a fibre laser is used. The laser beam is directly irradiated on the aluminum surface to ensure a power density high enough to generate a stable keyhole welding process, Solchenbach and Plapper (2013). For a better control of the temperature profile, beam oscillation is superposed to the linear feed direction as described in eq_1.

$$\begin{pmatrix} x_{(t)} \\ y_{(t)} \end{pmatrix} = \begin{pmatrix} a \cdot cos(2\pi f_x t + \varphi_x) + vt + a_0 \\ a \cdot sin(2\pi f_y t + \varphi_y) \end{pmatrix}$$

eq_1

with

a	amplitude [mm]
a_0	t = 0 [mm]
$f_{x,y}$	oscillation frequency in x and y direction [Hz]
v	feed rate [mm s^{-1}]
$\varphi_{x,y}$	phase angle in x and y direction [rad]

For the studies described in this report, the phase angles have been set to φx = −π and φy = 0 while the oscillation frequencies were chosen to $f_x = f_y$ = 500Hz. The resulting trajectory of the laser beam, as shown in figure 2, a), creates a spatially modulated power distribution.

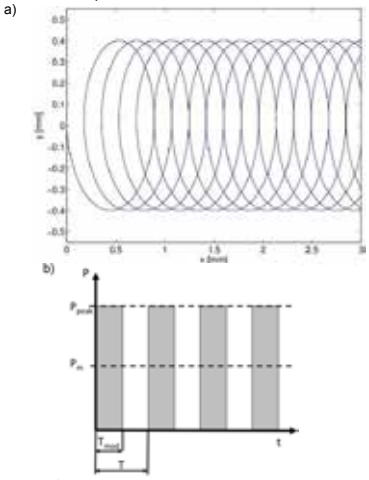

2_Power modulation, a) spatial modulation by superposed beam oscillation on the linear feed; b) pulse width modulation of the laser power

Additionally, time modulation of the laser beam is used to control the overall heat input. Figure 2, b) shows the principle of temporal power modulation of the laser beam which was set to a rectangular shape at a frequency of 1/T = *25kHz*. The modulated power can be computed according to equation (2), b).

$$P_m = \frac{T_{mod}}{T} \cdot P_{peak}$$

eq_2

with

P_{peak}	peak power [J s^{-1}]
P_m	modulated power [J s^{-1}]
T_{mod}	modulation time [ms]
1/T	modulation frequency [Hz]
t	time [s]

Experimental Setup

For the experiments, 0.5mm thick EN-AW1050A aluminum in half-hard state and 1.0mm thick polyamide PA6.6 samples were used in a aluminum-PA6.6-aluminum stack. The samples had a geometry of 60mm x 40mm and 150mm x 40mm for aluminum and PA, respectively and were arranged in overlap configuration with an overlap of 25mm. The polymer was cleaned with acetone. The aluminum was used in three different surface states:

_Set A (As delivered): the aluminum surface was degreased with acetone;
_Set B (Naturally oxidized): the aluminum surface was ablated by means of short pulsed laser ablation and a naturally oxide layer was formed;
_Set C (Anodized): The aluminum surface was anodized using phosphoric acid.

After laser beam joining over a length of 40mm, the samples were characterized by optical and electron microscopy. The formation of temperature in the joining area was measured by means of an infrared thermo-camera. The experimental setup for the thermographic measurements is shown in Fig.(3).

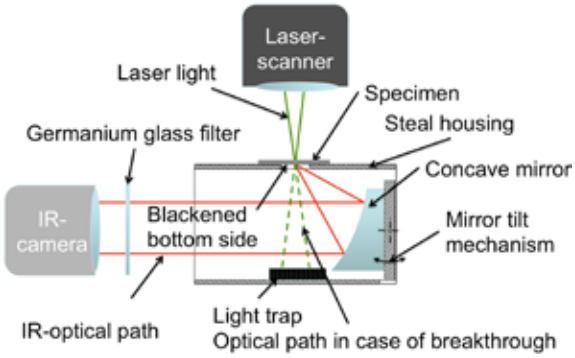

3_Experimental setup for temperature measurements

Tensile shear tests were conducted in order to analyze the impact of the surface treatment on the mechanical characteristics. Shear tests were performed within 18 hours, one week and one month ofter the joining operation to detect possible aging of the interface in ambient conditions. In order to prove the existence of hydrogen bridges, a Bruker Hyperion 2000 infrared spectroscopic device was used to analyze the samples after mechanical testing.
For the direct joining experiments, a single mode Trumpf TruFiber 400 fibre laser with a near-infrared wavelength of λ = 1070nm and a maximum power of P = 400W was used in combination with a Scanlab HS20 2D f-θ-scanner head. Thus, a spot diameter of 30µm can be obtained with the focus on the Al surface.

Results and Discussion

In this section, the experimental results are presented and discussed.
Table (1) gives an overview of the three sets of surface treatment compared regarding their effect on laser joining. After the treatment of the aluminum substrate, the

topological surface characteristic of all sets of samples was quantified which is represented by the arithmetic average roughness R_a in Table (1). The roughness measurement was executed in order to detect variations of the surface topology that might effect the maximum shear load due to unwanted mechanical interlocking.

Table 1. Different surface pre-treatments

Samples	Treatment applied	R_a
A	As delivered	0.468 µm
B	Naturally oxidized	1.127 µm
C	Anodized	0.142 µm

Comparing the results in Fig. (4) shows that the anodization process has smoothed existing imperfections, whereas the laser ablating has induced an increase of surface roughness. The latter can be explained by the transfer of the pulsed laser pattern to the substrate during laser ablation.

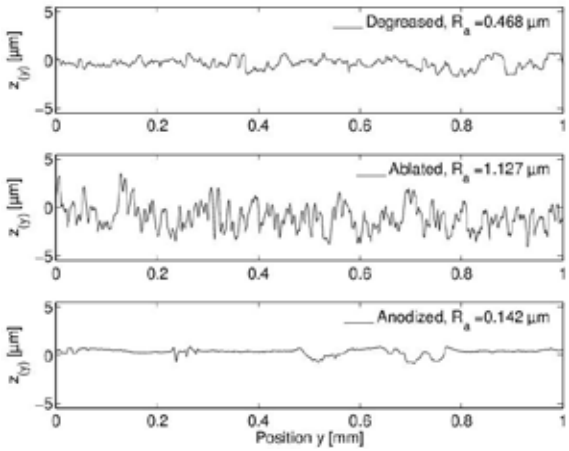

4_Surface topography

However, the impact of surface roughness in the micron and sub-micron scale on the mechanical properties of the hybrid joints can be neglected as the aspect ratio of surface roughness and the wavelength of the surface topology is smaller than 0.1 and a mechanical interlocking effect is insignificant. Therefore, purely physicochemical based bonding phenomena are expected, which will be proved in section 5.4.

Interface Charactization

With the help of the laser beam oscillation the heat input into the joining area was broadened without generating a deeper penetration of the laser beam into the thin aluminum sheet (Fig. (5), a)). The resulting melt bath of the metal approaches a well-defined rectangular shaped cross section. In this way a high amount of heat energy can be transferred into the aluminum from where it is transported to the interface region via heat conduction as shown in Fig. (5), a). The wetting of the polyamide on the substrate was measured at a width of 1.1 mm. A formation of bubbles in the polymer was not detected.

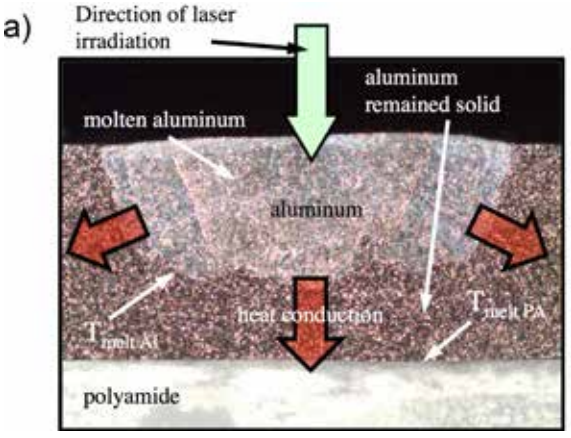

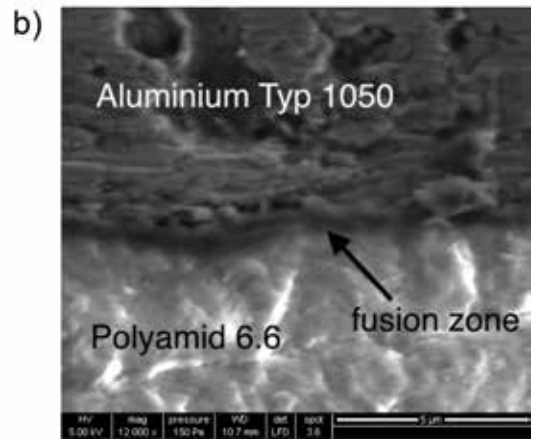

5_Cross sectional micrograph; a) optical microscopy, b) SEM microscopy

SEM analyses showed a tight bond between both dissimilar materials without indications of chemical decomposition, see Fig.(5), b). A fusion zone at the aluminum-polyamide-interface was detected which can be seen as a dark-grey band between both materials, see marker in Fig.(5), b). However, it is believed that the thickness of this fusion zone is overrated in the measurement. During the sample preparation process by mechanical polishing traces of PA might be wiped over the aluminum in the fusion zone which then seem thicker than it is.

Fig.(6) shows the evolution of the temperature at the interface during laser beam joining over time. A peak temperature of 345°C was measured which means that the melting temperature of the polyamide material was exceeded for 50ms. Decomposition temperature was not reached. As the measurement was performed with aluminum only the resulting peak temperature during the joining process is expected to be lowered with an attached polymer layer in overlap configuration. As the formation of gas bubbles was not detected, see Fig.(5), b), the effective temperature during joining was below 330°C. However, an thermographic measurement with polymer layer was not possible due to the low transmittance of the infrared light through the polymer.

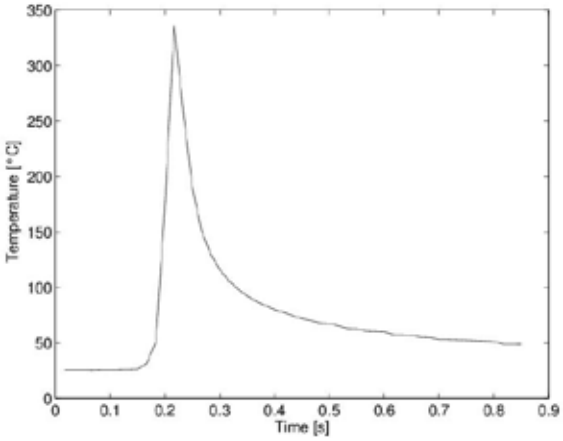

6_Temperature evolution at the joint interface

Mechanical Characteristics

For optimal process parameters, a maximum shear load of 1600N was measured on the ablated and naturally oxidized samples (modulated power = 300W), see Fig.(7). The samples failed in the polyamide base material next to the joint area (cohesive failure). With decreasing energy input (modulated power < 300W), the shear load decreased strongly and the samples failed at the aluminum-polyamide interface. For higher energy input, the shear strength was also reduced but, however, with a smaller gradient. Also here, the samples failed at the interface. For the latter case (modulated power > 300W), also chemical degradation of the polyamide layer by means of bubble formation at the interface was detected. The high gas pressure in the bubbles partially separated the PA melt from the substrate during resolidification which reduced the effective contact area.

This analysis highlights that the energy input into the fusion zone is of atmost importance in order to achieve optimal mechanical joint characteristics and to avoid chemical degradation of the polymer.

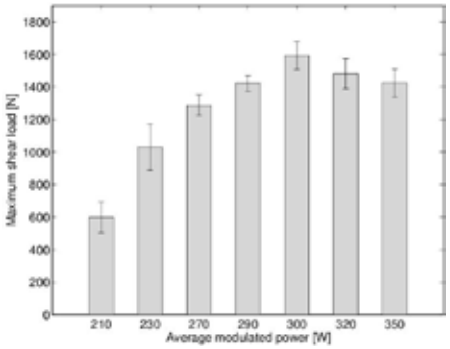

7_Maximum shear load depending on modulated power

From Fig.(8) it can be seen that the shear strength of the hybrid metal-polymer joints is strongly dependent on the pre-treatment of the aluminum surface. The "as-delivered" condition (A) features lowest strength. Despite the samples were cleaned with acetone before joining, contamination of the surface with aliphatic hydrocarbons or other pollutants accumulated during the manufacturing process cannot be excluded. After aging, the strength was diminished by 31 % after one week and 64% after one month. Although the substitution of hydrogen bonds at the interface by deposition of H2O molecules is expected to be the reason for these effects a subsequent FTIR-analysis of the polymer could not confirm this hypothesis. The root cause for this behavior remains unresolved and will be subject of future investigations. After laser ablation and the formation of a naturally grown oxide layer (B), the shear strength increased by a factor of 4. Aging effects after one week and one month, respectively, were not detected. Furthermore, the standard deviation of the strength is significantly lower which indicates a high process and bond stability.

The anodized aluminum samples (C) also showed good shear strength results but, however, with a high standard deviation which can be explained by the effects of the anodisation layer on the heat transfer behavior of the aluminum surface, Lee et al. (2013). Also here, aging did not affect the shear strength significantly.

Infrared Spectroscopy

After fracture a FTIR-spectroscopic analysis of the polyamide was performed. The spectra from the joined samples were compared with a reference spectrum which was taken on the polyamide base material in order to detect a physicochemical interaction at the aluminum-polyamide fusion zone and to show an effect of the different surface treatments.

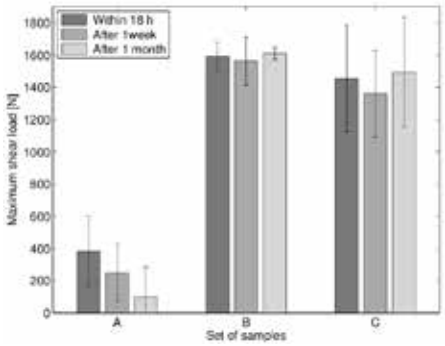

8_Shear load for variation of the Al surface treatment

Fig.(9) shows the spectra of sample set B (ablated and naturally oxidized) after joining. A reduced absorption at wavenumbers 3300cm^{-1}, 1633cm^{-1} and 1539cm^{-1}, representing N-H stretch, C=O stretch and N-H bending + C-N stretch, was detected, Domininghaus et al. (2012). As a change of molecular constitution can be excluded, this effect induces that the extra-molecular structures have re-arranged which may be a sign of crystallization germs at the interface between the adjoining materials. The IR fingerprints of sample set C did not exhibit a significant variation to the sample set B whereas the measurements of sample set A did not vary from the reference spectrum at all. Higher shear strength was measured for sample sets B and C in comparison to set A which correlates with a stronger physicochemical interaction, visible by increasing reduction of absorption in the IR spectra.

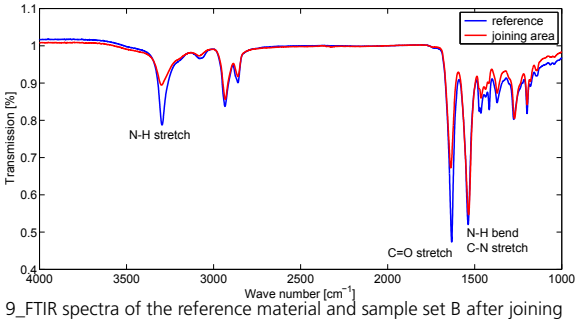

9_FTIR spectra of the reference material and sample set B after joining

As the formation of hydrogen bridges cannot be measured directly, the observed phenomena cannot be taken as evidence for the existence of the assumed interactions between the amide-groups of the polyamide, consisting of covalent bonds, and the ionic Al_2O_3 present in the boundary layer of the aluminum substrate. They indicate an interaction with dependence on the pre-conditioning which is plasticized in the IR-fingerprint of the molten polymer after resolidification and can be assigned to the predicted position at the polyamide molecule, Briehl (2008).

Conclusions

A novel laser beam joining process for hybrid polyamide-aluminum structures was reported. The spatial and temporal heat input was tailored for optimal bonding quality. At the interface it was proven that the polyamide was not decomposed as a result of excessive thermal stress. It was shown that mechanical or electro-chemical surface pre-treatment of the aluminum substrate has a distinctive effect on the shear strength. However, the bond quality did not correspond with a change of surface roughness. Therefore, mechanical interlocking by means of surface topology of the pretreated substrate was not the principal cause for the bonding mechanism. Chemical analysis by means of IR-spectroscopy has shown a physicochemical interaction based on hydrogen bonds.

In future work, the exact physicochemical changes of the polymer at the interface between both materials has to be studied in detail in order to gain a fundamental understanding of the effects during the laser joining process.

Acknowledgements

The authors would like to thanks the CRP Tudor AMS group for their great support on the treatment of the aluminum surfaces and the SEM measurements.

www.uni.lu

REFERENCES

Amend, P., Pfindel, S., Schmidt, M., 2013. Thermal joining of thermoplastic metal hybrids by means of mono- and polychromatic radiation. Technical Report. Bayerisches Laserzentrum GmbH.

Balle, F., Emrich, S.,Wagner, G., Eifler, D., 2008. Fugen artfremderWerkstoffe – Ultraschallschweißen von Kohlenstofffasertextilien mit Metallen. MP Materials Testing 50.

Briehl, H., 2008. Chemie der Werkstoffe. 2 ed., Teubner.

Brockmann, H., 1987. Chemical Aspects of Adhesion between Metals and Polymers. The Journal of Adhesion 22, 71–76.

Domininghaus, H., Elsner, P., Eyerer, P., Hirth, T., 2012. Kunststoffe - Eigenschaften und Anwendungen. 8 ed., Springer Verlag.

Farazila, Y., Miyashito, Y., Hua, W., Mutoh, Y., Otsuka, Y., 2011. Yag laser spot welding of pet and metallic materials. JLMN-Journal of Laser. Micro/Nano Engineering 6, 69–74.

Flock, D., 2011. W¨armeleitungsf¨ugen Hybrider Kunststoff-Metall-Verbindungen. Ph.D. thesis. Fakult¨at f¨ur Maschinenwesen der Rheinisch- Westfälischen Technischen Hochschule Aachen.

Fortunato, A., Cuccolini, G., Ascari, A., Orazi, L., Campana, G., Tani, G., 2010. Hybrid Metal-Plastic Joining by Means of Laser. Technical. Report. University of Bologna and University of Modena.

Jung, K.W., Kawahito, Y., Takahashi, M., Katayama, S., 2013. Laser direct joining of carbon fiber reinforced plastic to aluminum alloy. Journal of Laser Applications 25.

Katayama, S., Kawahito, Y., 2008. Laser direct joining of metal and plastic. Scripta Materialia 59, 1247–1250.

Kelly, G., 2004. Joining of Carbon Fibre Reinforced Plastics for Automotive Applications. Ph.D. thesis. Royal Institute of Technology - Sweden.

Klein, B., 2013. Leichtbau-Konstruktion: Berechnungsgrundlagen und Gestaltung (German Edition). Springer Vieweg.

Lee, J., Kim, Y., Jung, U., Chung, W., 2013. Thermal conductivity of anodized aluminum oxide layer: The effect of electrolyte and temperature. Materials Chemistry and Physics 141, 680–685.

Michaeli, W., Hoffmann, W.M., 2009. Hybride Verbindungen. Kunststoffe , 50–53.

Mitschang, P., Velthuis, R., 2008. Process Parameters for Induction Welding of Metal/Composite Joints. Technical Report. Institut f¨ur Verbundwerkstoffe GmbH Kaiserslautern.

Nikolova, D., 2005. Charakterisierung und Modifizierung der Grenzfl¨achen im Polymer-Metall-Verbund. Ph.D. thesis. Martin-Luther-Universität Halle-Wittenberg.

Roesner, A., Scheik, S., Olowinsky, A., Gillner, A., Schleser, U.R.M., 2011. Laser Assisted Joining of Plastic Metal Hybrids. Technical Report. Fraunhofer Institute for Laser Technology, Welding und Joining Institute, RWTH Aachen University.

Solchenbach, T., Plapper, P., 2013. Mechanical characteristics of laser braze-welded aluminium-copper connections. Optics & Laser Technology 54, 249–256.

Wahba, M., Kawahito, Y., Katayama, S., 2011. Laser Direct Joining of AZ91D thixomolded Mg Alloy and Amorphous Polyethylene Terephthalate. Journal of Material Processing Technology 211, 1166–1174.

Wirth, F.X., 2011. Mischverbindungen durch R¨uhrreibschweißen - F¨ugen von Aluminiumstrangpressprofilen. wt Werkstatttechnik online Bd. Jahrgang 101.

Permanent-Magnetsynchronmotoren (PMSM) wurden seit langem in Servoantriebe eingesetzt und werden in letzter Zeit zunehmend in vielen Bereichen der Industriellen Antriebstechnik verwendet. Ein anderer Anwendungsbereich für die PMSM ist das Elektrofahrzeug. Grund dafür ist der Fortschritt der Mikro-und Leistungselektronik, der die Einführung auf dem Markt von kostengünstigen, kompakten und leistungsfähigen Systemlösungen ermöglicht hat. Ferner ist die PMSM gegenüber der bürstenhaften Gleichstrommaschine kleiner und robuster. Durch den Wegfall der Bürsten erhöht sich nicht nur die Lebensdauer des Antriebes, sondern auch die Geräusche werden vermindert[4].

UNIVERSITÉ DU LUXEMBOURG

Lauréat du Prix de la Revue Technique Luxembourgeoise 2014

FELDORIENTIERTE REGELUNG EINES PERMANENT-MAGNET-SYNCHRONMOTORS IN LABVIEW_

Mithat Basli

Das optimale Verfahren für die Regelung der PMSM ist die feldorientierte Regelung, wobei die Maschinengrößen in drehmoment- und flussbildende Komponenten zerlegt werden. Dadurch wird eine technische Entkopplung der Maschinenzustände erreicht, wie bei der Gleichstrommaschine. Daraus resultieren ähnlich wie bei den Gleichstrommaschinen gute und einfache Regelungseigenschaften.

Permanent Magnetsynchronmaschine

Permanent Magnetsynchronmotor ist eine rotierende elektrische Maschine. Der Ständer enthält drei Phasenwicklungen, während der Rotor mit einem Permanentmagnet versehen ist. Das Luftspalt- Magnetfeld wird durch diesen Permanentmagnet erzeugt und daher kann konstant angenommen werden. Beim konventionellen Gleichstrommotor kommt die Kommutierung durch einen mechanischen Kommutator zustande, die PMSM hingegen benötigt für die Richtungssteuerung des Stroms durch die Statorwicklungen einen elektrischen Kommutator. Da die PMSM die Ankerspulen am Stator haben, ist ein externer Schaltkreis notwendig, um die Kommutierung zu gewährleisten. Zu diesem Zweck wird die B6-Dreiphasen-Wechselrichter-Topologie verwendet[3].

Das Drehmoment, das durch die Wechselwirkung zweier Magnetfelder entsteht, bringt den Motor zum Drehen. Im Permanent-Magnetmotor wird eins der Magnetfelder vom Permanentmagnet erzeugt und das andere von Statorwicklungen. Das maximale Drehmoment entsteht, wenn der magnetische Vektor des Rotors senkrecht zu dem magnetischen Vektor des Stators liegt.

Der Permanent-Magnetsynchronmotor, der im Rahmen dieser Arbeit geregelt werden sollte, wurde von Prof. Dr. Ing. Jean-Régis Hadji Minaglou entworfen. In Tabelle 1 werden die Maschinendaten dargestellt[1].

	PMSM-Daten	Einheit
Längsinduktivität	0.002744039	H
Querinduktivität	0.002222237	H
Widerstand	0.057151785	Ω
Polpaarzahl	2	-
Rotorträgheit	0.035866	$kg.m^2$
Fluß des Permanentmagnets	0.414	Wb
Nennstrom	109	A
Nennspannung	270	V
Nenndrehzahl	2700	rpm
Nenndrehmoment	92.55	Nm
Nennleistung	25	kW

_Maschinen Daten

Feldorientierte Regelung

Im Gleichstrommotor sind die Fluss- und Drehmoment bildenden Ströme senkrecht zueinander und können daher

unabhängig voneinander geregelt werden. Das Drehmoment wird durch die folgende Gleichung definiert[3].

$$T_e = K_a \varnothing I_a$$

Wobei K_a Maschinenkonstante, Erregerfluss und I_a Ankerstrom sind.

Durch die Permanentmagnete ist der Erregerfluss konstant, also dann wird das Drehmoment nur über den Ankerstrom geregelt. Bei Gleichstrommaschinen spricht man von Entkopplung der Fluss- und Drehmoment bildenden Ströme. Dadurch wird es möglich, den Fluss und das Drehmoment getrennt zu regeln.

Bei Drehstrommaschinen sind das Stator Feld und das Rotor Feld nicht orthogonal zueinander. Der einzige Strom, der geregelt werden kann, ist der Stator Strom. Die feldorientierte Regelung ist die Methode, die verwendet wird, um die technische Entkopplung der Fluss- und Drehmomentregelung zu erreichen. Dabei werden die Stator Ströme (drei Phasenströme) durch die Clarke - und Park Transformation in Drehmoment und Fluss bildende Komponenten zerlegt.

Die feldorientierte Regelung hat die folgenden Vorteile.
_Transformation eines komplexen und gekoppelten AC-Modells in ein einfaches und lineares System.
_Unabhängige Kontrolle vom Fluss und Drehmoment ähn lich wie beim DC-Motor.
_Hoher Wirkungsgrad
_Großer Drehzahlbereich durch die Feldschwächung.

Der Querschnitt einer zwei-poligen permanenterregten Synchronmaschine wird in Figur 1 dargestellt [2].

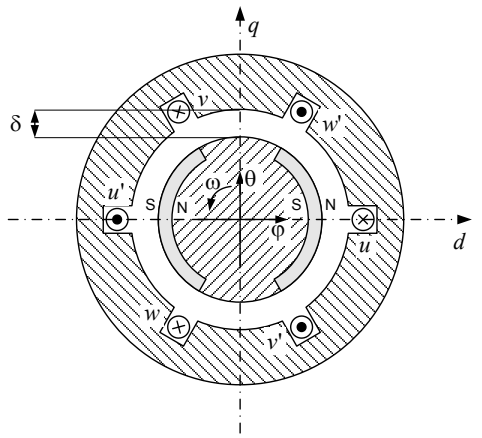

_Querschnitt einer zwei-poligen permanenterregten Synchronmaschine

Das Ersatzschaltbild der Synchronmaschine lässt sich wie in Figur 2 aufgezeigt darstellen [2].

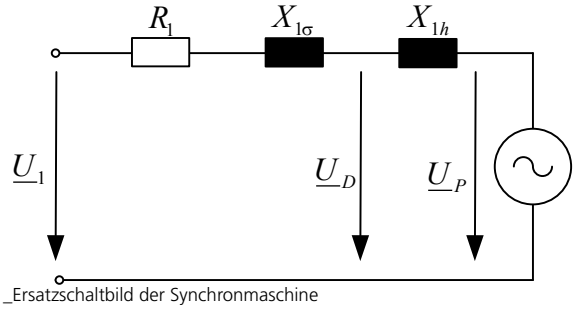

_Ersatzschaltbild der Synchronmaschine

mit:
$\underline{U}_1$: Ständerspannung
R_1: Ständerwiderstand
$X_{1\sigma}$: Ständerstreureaktanz
$\underline{U}_D$: Drehfeldspannung
X_{1h}: Hauptreaktanz
$\underline{U}_P$: Polradspannung

Es gelten folgende Definitionen:

i_d: Ständerlängsachse, Blindstrom
i_q: Ständerquerachse, Wirkstrom
φ: Läuferlängsachse, Permanentmagnete

Die elektrische Winkelgeschwindigkeit des Läufers ist gegeben wie folgt:

$$\omega = \frac{d\gamma}{dt} = 2\pi p n$$

Wobei p die Polpaarzahl ist.
Das folgende Koordinatensystem wird ausgewählt:

$$\frac{d\rho}{dt} = \frac{d\gamma}{dt}$$

Durch die Clarke – und Park Transformation wird die Auslegung des Stromreglers einfacher. Damit liegt die Bezugsachse d in der imaginären Achse und q in der reellen Achse. Für Motorbetrieb gilt das Verbraucherzählpfeilsystem. Es kann ausgehend von den dynamischen Gleichungen der Zweiachsentheorie das folgende Gleichungssystem schreiben:

$$u_d = R_s i_d + \frac{d\psi_d}{dt} - \omega\psi_q$$

$$u_q = R_s i_q + \frac{d\psi_q}{dt} + \omega\psi_d$$

$$\psi_d = L_d i_d + \varphi$$

$$\psi_q = L_q i_q$$

$$M_{el} = p(i_q\psi_d - i_d\psi_q) = M_w + \frac{J}{p}\frac{d\omega}{dt}$$

wobei:

φ : Längs- und Querflussverkettungen

R_S: Stator-Widerstand

u_d, u_q : Längs- und Querspannungen

M_{el}: Elektromagnetisches Drehmoment

M_W: Lastmoment

J: Rotorträgheit

Mit den Zeitkonstanten

$$T_d = \frac{L_d}{R_s},\ T_q = \frac{L_q}{R_s}$$

erhält man das Differentialgleichungssystem, mit dem der permanenterregte Synchronmotor mit Polradlagergeber vollständig beschrieben wird.

$$T_d\frac{di_d}{dt} + i_d = \frac{u_d}{R_s} + \omega T_q i_q$$

$$T_q\frac{di_q}{dt} + i_q = \frac{u_q}{R_s} - \omega T_d\left(i_d + \frac{\varphi}{T_d}\right)$$

$$\frac{J}{p}\frac{d\omega}{dt} = pL_d\left(\frac{\varphi}{L_d} - i_d\left(\frac{L_q}{L_d} - 1\right)\right)i_q - M_w$$

Die Steuerung der Maschine erfolgt so, dass im Normalbetrieb die Ankerdurchflutung und das Erregerfeld senkrecht aufeinander stehen. Dies bedeutet, wenn der Fluss der Permanenterregung durch dargestellt wird, dass der Ständerstrom keine Längskomponente hat, d.h. und die Querkomponente die drehmomentbildende Komponente ist. Dann gilt für die Spannung:

$$\frac{u_d}{R_s} + \omega T_q i_q = 0 \text{ bzw. } u_d = -\omega L_q i_q$$

Bei der Auslegung des Stromreglers wird vorausgesetzt, dass die Differenz zwi¬schen der elektrischen und der mechanischen Zeitkonstante groß ist. Diese Annahme ist gültig, weil die Massenträgheit des Maschinenläufers groß ist. Das dynamische Modell wird dann vereinfacht, weil die Drehzahl innerhalb eines Abtastschrittes als konstant angenommen werden kann.
In Figur 3 wird das Strukturbild der feldorientierten Regelung des PMSM Motors mit kaskadierter Drehzahl-Regelung dargestellt [2].

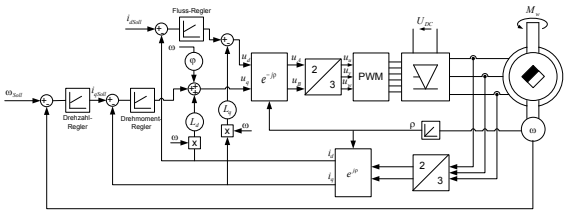

_Strukturbild der feldorientiertgeregelten PMSM mit kaskadierter Drehzahl-Regelung

Im Rahmen dieser Arbeit werden Drehzahl- und Flussregelung weggelassen und es wird nur die Drehmomentregelung vorgesehen. In Figur 4 wird die vereinfachte Struktur zur Drehmomentregelung dargestellt.

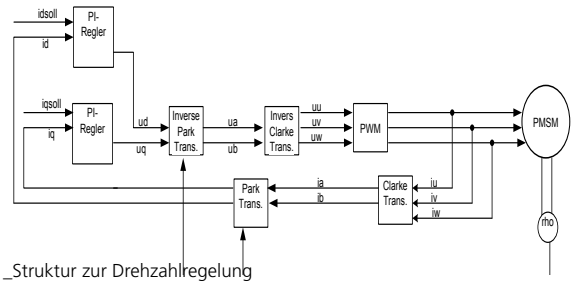

_Struktur zur Drehzahlregelung

Datenerfassung und Messungen

Für die feldorientierte Regelung ist die Erfassung der Rotorlage notwendig. Mit Hilfe des Polradwinkels werden die Park- und Inverse Park Transformationen gemacht. Für die Ermittlung der Rotorlage wurde ein inkrementaler Drehgeber verwendet. Des Weiteren werden die Phasenströme i_u, i_v und i_w benötigt. Für die Stromerfassung wurden Hall-Sensoren benutzt.

Funktionsweise des Regelkreises

Die Phasenströme i_u, i_v und i_w werden mittels Hall-Sensoren erfasst. Durch die Clarke- Transformation werden die Dreiphasenströme in ein orthogonales Phasensystem i_a und i_b umgewandelt. Danach erfolgt die Park-Transformation, bei der die Phasenströme auf ein mit dem Fluss rotierenden Koordinatensystem transformiert werden. Die Park-Transformation benötigt den Rotorwinkel rho. Die Ausgänge der Park-Transformation sind die Ströme i_d und i_q. Diese Ströme werden über zwei PI-Regler geregelt. Die Stellgrößen der PI-Regler sind die Spannungen U_d und U_q. Über die Inverse-Park- und Clarke –Transformationen wird das Zweiphasensystem ins Dreiphasensystem zurück transformiert. Anschließend werden die IGBTs über die Pulsweiten-modulation gesteuert und damit ist der Kreis geschlossen.

Messungen

Als Beweis, dass die PI-Regler richtig funktionieren, wurden Messungen vorgenommen. Die Ausgänge der PI-Regler sind die Spannungen u_d und u_q. Für die Sollwerte i_d=0A und i_q=2A=0,16V(2/12,5) werden die Stellwerte u_d und u_q sowie die Rotordrehzahl (rpm) der PMSM in Figur 5 dargestellt.

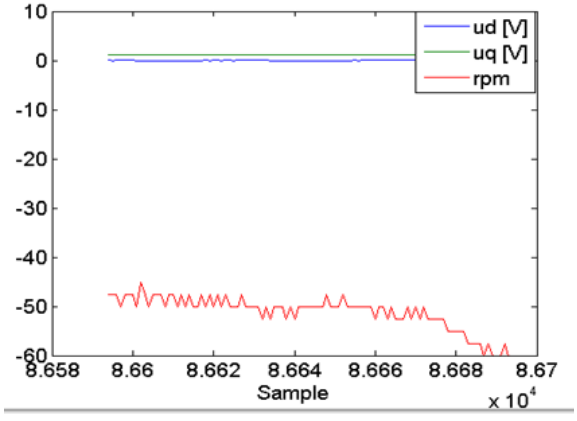

_Die Stellwerte u_d und u_q für die Stromsollwerte i_d=0A und i_q=2A

Im Leerlauf u_q=w*Ø, wobei w=2ϖn=(2*ϖ*55)/60= 5,75(1/s) und Ø=0,323Vs sind. Daraus gibt es sich für die Spannung u_q=1,86 V.

Für die Sollwerte der Ströme i_d=0A und i_q=-2A= -0,16V werden die Stellwerte u_d und u_q in Figur 6 dargestellt.

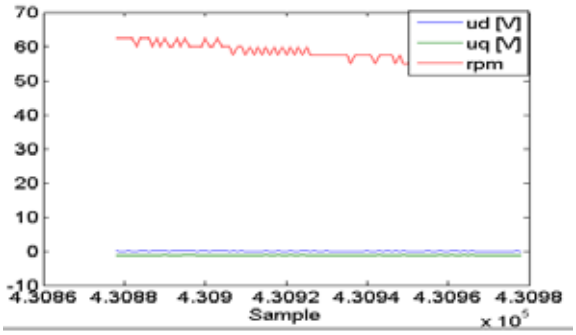

_Die Stellwerte u_d und u_q für die Stromsollwerte i_d=0A und i_q=-2A

Wie in Figuren 5 und 6 aufgezeigt, die Ausgänge der PI-Regler stimmen mit den Erwartungen überein. Für den positiven Sollwert von i_q ist der Stellwert von u_q auch positiv und für den negativen Sollwert von i_q ist der Stellwert von u_q negativ.

Für die Kontrolle, ob die PI-Regler die Ströme i_d und i_q richtig regeln, wurden auch Messungen vorgenommen. In Figur 7 werden die Strom-Istwerte $i_{dfilterist}$ und $i_{qfilterist}$ für die Stromsollwerte i_{dsoll}=0A und i_{qsoll}=3A = 0,24V dargestellt.

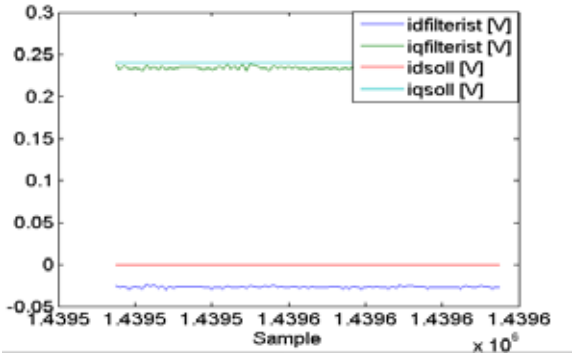

_Strom-Istwerte $i_{dfilterist}$ und $i_{qfilterist}$ für die Stromsollwerte i_{dsoll}=0A und i_{qsoll}=-3A=-0,24V

In Figur 8 werden die Strom-Istwerte $i_{dfilterist}$ und $i_{qfilterist}$ für die Stromsollwerte i_{dsoll}=0A und i_{qsoll}=-3A= -0,24V dargestellt.

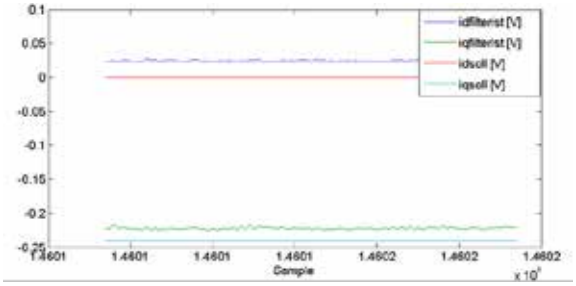

_Strom-Istwerte $i_{dfilterist}$ und $i_{qfilterist}$ für die Stromsollwerte i_{dsoll}=0A und i_{qsoll}=3A=0,24V

Wie in Figuren 7 und 8 dargestellt, regeln die PI-Regler die Ströme nicht richtig. Die Regelabweichung basiert darauf, dass nur der P-Anteil des Stromreglers implementiert ist.

Für den Ausgleich des Stationären Fehlers muss auch der I-Anteil eingesetzt werden. Darüber hinaus muss noch ein Drehzahlregler implementiert werden, damit der Motor nicht wegläuft, wenn er nicht belastet ist.

Zusammenfassung
Bei der vorliegenden Arbeit handelt es sich um die feldorientierte Regelung der Permanent-Magnet Synchronmaschine mit LabVIEW. Die Phasenströme i_u und i_v, sowie die Rotorlage sind für die Regelung notwendig und können problemlos erfasst werden. Da die Phasenströme mit Verzerrungen behaftet sind, ist ein Filter erforderlich.

Der Wechselrichter hat einen Einfluss auf die Gleichspannungsquelle. Um den Einfluss des Wechselrichters zu beseitigen, wurde ein Zwischenkreiskondensator auf der Gleichspannungsseite angeschlossen. Der Zwischenkreiskondensator kompensiert die Verzerrungsleistung, die aufgrund der Pulsweitenmodulation auftritt.

Die Pulsweitenmodulation funktioniert richtig, solange der elektrische Winkel (die Rotorlage) vorhanden ist. Bei kleinen Gleichspannungen ebenso wie bei niedrigen Frequenzen der Sinussignale sind die Induzierte Spannung und damit die magnetische Feldstörung klein. Ist die magnetische Feldstörung klein, dann wird die Rotorlage richtig erfasst. Erhöht man die Gleichspannungsquelle oder die Frequenz der Sinussignale, dann wird die magnetische Feldstärke derart stark, dass die Inkremental Drehgeber gestört wird. Demzufolge wird die Rotorlage nicht mehr richtig ermittelt.

Die beiden Regler wurden getestet und funktionieren richtig. Für die feldorientierte Regelung der PMSM muss die Rotorlage erfasst werden. Wie bei der PWM verschwindet das Signal der Rotorlage, wenn man den Sollwert von i_q erhöht. Die Maschine erzeugt so ein starkes Magnetfeld. Dies stört die ganze Elektronik, sodass die Signale nicht mehr ausgewertet werden können. Des Weiteren ist die Konstruktion, die für die PWM erforderlich ist, nicht zuverlässig.

Damit die Regelung der PMSM möglich ist, muss entweder die ganze Elektronik gegen das Magnetfeld isoliert oder eine Sensorlose Regelung durchgeführt werden. Des Weiteren ist die Konstruktion für die PWM zu verbessern.

www.uni.lu

Literaturverzeichnis

1_Jean-Régis Hadji-Minaglou: ´´Antriebskonzepte mit permanenterregten Synchronmotoren für den Einsatz im Elektrofahrzeug´´, Verlag Shaker.

2_Jean-Régis Hadji-Minaglou: ´´Leistungselektronik 1,2,3´´, Skriptum zur Vorlesung, Universität Luxemburg.

3_http://www.microsemi.com/document-portal/doc_view/130909-sf-foc-pmsm-hall-ug?ml=1

4_http://www.db-thueringen.de/servlets/DerivateServlet/Derivate-13770/ilm1-2007000172.pdf

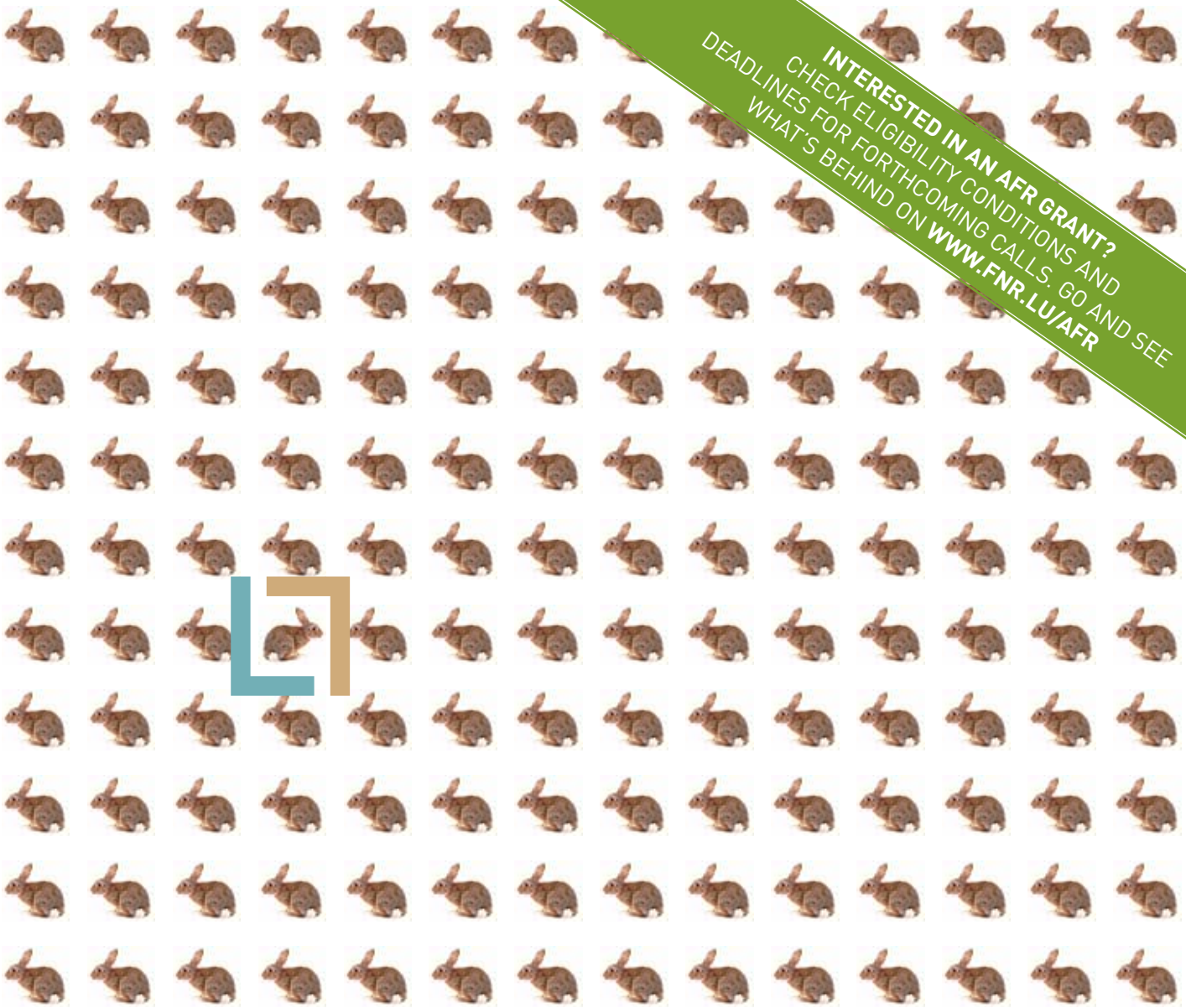

INTERESTED IN AN AFR GRANT?
CHECK ELIGIBILITY CONDITIONS AND DEADLINES FOR FORTHCOMING CALLS. GO AND SEE WHAT'S BEHIND ON **WWW.FNR.LU/AFR**

PhD and Postdoc Grants for Public-Private Partnerships
See what's behind.

The FNR provides *Aides à la Formation-Recherche* (AFR) grants for PhD and postdoctoral research training. Next to offering PhD grants for research projects carried out in public research institutions in Luxembourg or abroad, the FNR strongly encourages doctoral and postdoctoral research projects performed as public-private partnerships (PPP) with accredited companies in Luxembourg. The salary of the PhD or postdoc researcher who will work on a research project as a member of the company's staff will be paid through the AFR-PPP grant scheme.

In order to benefit of the financial support for PPP under AFR, an innovative research project needs to be developed jointly by the PhD/postdoc candidate, the company and a public sector higher education or research institution in Luxembourg or abroad. For postdocs, an international or intersectoral mobility is mandatory.

Interested in hosting an AFR fellow during his or her PhD or Postdoc training? Go and see what's behind on **www.fnr.lu/afr-ppp** or send an email to **afr@fnr.lu**.

AFR
FUNDING SCHEME
FOR PHDS AND POSTDOCS
(AIDES À LA FORMATION-RECHERCHE)

Fonds National de la Recherche Luxembourg
INVESTIGATING FUTURE CHALLENGES